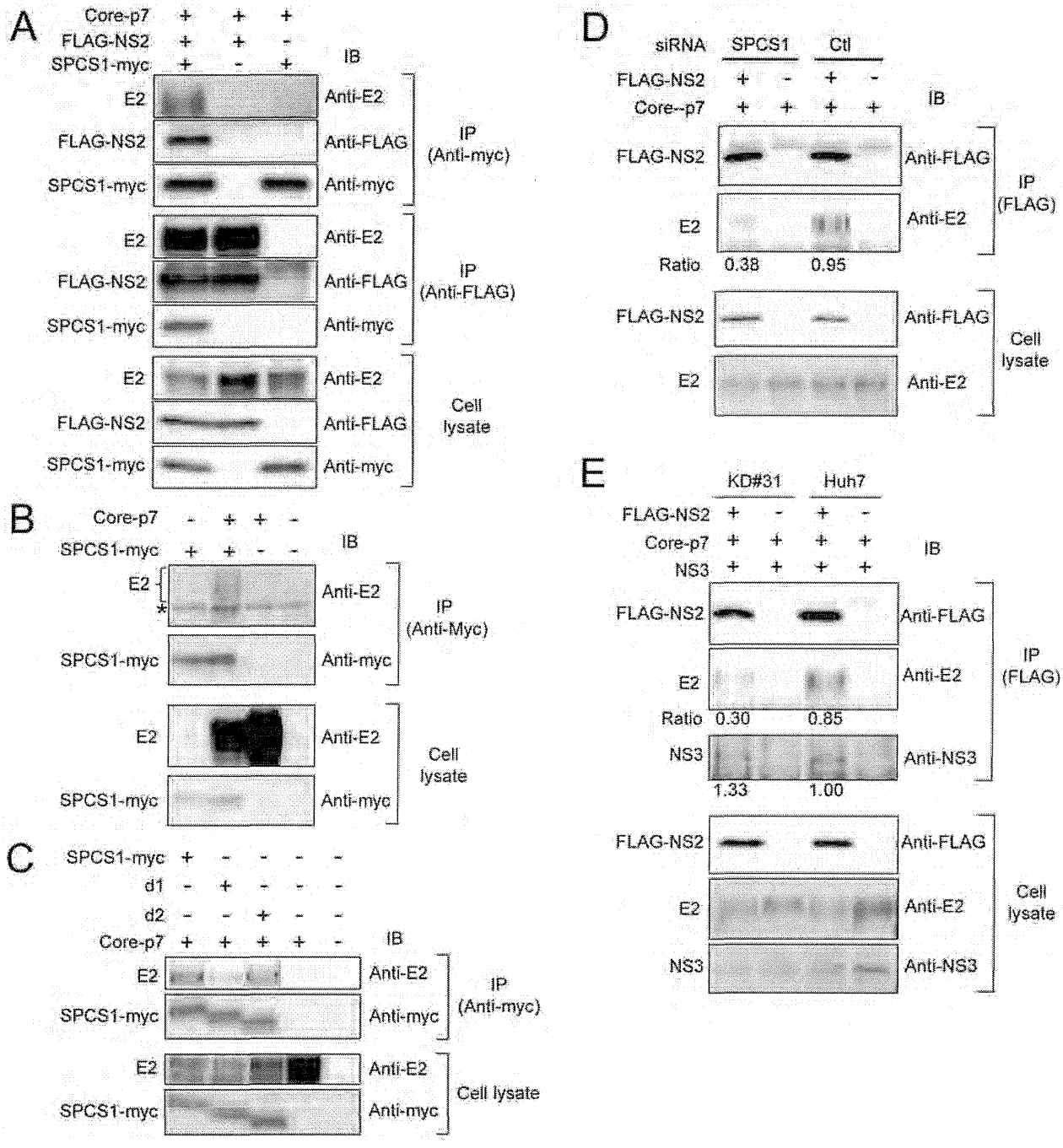


**Figure 6. SPCS1 forms a complex with NS2 and E2.** (A) Lysates of cells, which were co-transfected with Core-p7, FLAG-NS2, and SPCS1-myc expression plasmids, were immunoprecipitated with anti-myc or anti-FLAG antibody. The resulting precipitates and whole cell lysates used in IP were examined by immunoblotting using anti-E2, anti-FLAG, or anti-myc antibody. An empty plasmid was used as a negative control. (B) Cells were transfected with Core-p7 expression plasmid in the presence or absence of SPCS1-myc expression plasmid. The cell lysates of the transfected cells were immunoprecipitated with anti-myc antibody. The resulting precipitates and whole cell lysates used in IP were examined by immunoblotting using anti-E2 or anti-myc antibody. An empty plasmid was used as a negative control. The bands corresponding to immunoglobulin heavy chain are marked by an asterisk. (C) Cells were co-transfected with Core-p7 and SPCS1-myc expression plasmids. The cell lysates of the transfected cells were immunoprecipitated with anti-myc antibody. The resulting precipitates and whole cell lysates used in IP were examined by immunoblotting using anti-E2 or anti-myc antibody. (D) Huh7.5.1 cells were transfected with SPCS1 siRNA or control siRNA at a final concentration of 20 nM. After 24 h, Huh7.5.1 cells were then co-transfected with FLAG-NS2 and Core-p7 expression plasmids. The lysates of transfected cells were immunoprecipitated with anti-FLAG antibody, followed by immunoblotting with anti-FLAG and anti-E2 antibodies. Immunoblot analysis of whole cell lysates was also performed. Intensity of E2 bands was quantified, and the ratio of immunoprecipitated E2 to E2 in cell lysate was shown. Similar results were obtained in 2 independent experiments. (E) KD#31 cells and parental Huh-7 cells were co-transfected with FLAG-NS2, Core-p7, and NS3 expression plasmids. The lysates of transfected cells were immunoprecipitated with anti-FLAG antibody followed by immunoblotting with anti-FLAG, anti-E2, and anti-NS3 antibodies. Immunoblot analysis of whole cell lysates was also performed. The ratio of immunoprecipitated E2 or NS3 to E2 or NS3 in cell lysate, respectively, were shown.

doi:10.1371/journal.ppat.1003589.g006

nucleus [37]. They further screened a human liver cDNA library using NS2 with deletion of the N-terminal TM domain, and CIDE-B protein, a member of the CIDE family of apoptosis-inducing factors, was identified. However, whether CIDE-B is involved in the HCV lifecycle and/or viral pathogenesis is unclear. de Chassey et al. reported several cellular proteins as potential NS2 binding proteins using NS2 with N-terminal deletion as a bait [38]. Involvement of these proteins in the HCV lifecycle is also unclear. In our study, to screen for NS2-binding partners using full-length NS2 as a bait, we utilized a split-ubiquitin yeast two-hybrid system that allows for the identification of interactions between full-length integral membrane proteins or between a full-length membrane-associated protein and a soluble protein [39]. SPCS1 was identified as a positive clone of an NS2-binding protein, but proteins that have been reported to interact with NS2 were not selected from our screening.

SPCS1 is a component of the signal peptidase complex that processes membrane-associated and secreted proteins in cells. The mammalian signal peptidase complex consists of five subunits, SPCS1, SPCS2, SPCS3, SEC11A, and SEC11C [27]. Among them, the functional role of SPCS1 is still unclear, and SPCS1 is considered unlikely to function as a catalytic subunit according to membrane topology [40]. The yeast homolog of SPCS1, Spc1p, is also known to be nonessential for cell growth and enzyme activity [28,41]. Interestingly, these findings are consistent with the results obtained in this study. Knockdown of SPCS1 did not impair processing of HCV structural proteins (Fig. 4A) or secretion of apoE and albumin (Fig. 4B and C), which are regulated by ER membrane-associated signal peptidase activity. The propagation of JEV, whose structural protein regions are cleaved by signal peptidase, was also not affected by the knockdown of SPCS1 (Fig. 3B). SPCS1, SPCS2, and SPCS3 are among the host factors that function in HCV production identified from genome-wide siRNA screening [42]. It seemed that knockdown of SPCS1 had a higher impact on the later stage of viral infection compared to either SPCS2 or SPCS3, which are possibly involved in the catalytic activity of the signal peptidase.

Further analyses to address the mechanistic implication of SPCS1 on the HCV lifecycle revealed that SPCS1 knockdown impaired the assembly of infectious viruses in the cells, but not cell entry, RNA replication, or release from the cells (Fig. 5). We thus considered the possibility that the SPCS1-NS2 interaction is important for the role of NS2 in viral assembly. Several studies have reported that HCV NS2 is associated biochemically or genetically with viral structural proteins as well as NS proteins [10,18–25]. As an intriguing model, it has been proposed that NS2 functions as a key organizer of HCV assembly and plays a key role in recruiting viral envelope proteins and NS protein(s) such as NS3 to the assembly sites in close proximity to lipid droplets [21]. The interaction of NS2 with E2 has been shown by use of an HCV genome encoding tagged-NS2 protein in virion-producing cells. Furthermore, the selection of an assembly-deficient NS2 mutation located within its TM3 for pseudoreversion leads to a rescue mutation in the TM domain of E2, suggesting an in-membrane interaction between NS2 and E2 [21]. Another study identified two classes of NS2 mutations with defects in virus assembly; one class leads to reduced interaction with NS3, and the other, located in the TM3 domain, maintains its interaction with NS3 but shows impaired interaction between NS2 and E1-E2 [20]. However, the precise details of the NS2-E2 interaction, such as direct protein-protein binding or participating host factors, are unknown. Our results provide evidence that SPCS1 has an important role in the formation of the NS2-E2 complex by its interaction with both NS2 and E2, most likely via their transmembrane domains, including TM3 of NS2. As knockdown of SPCS1 reduced the interaction of NS2 and E2 as shown in Fig. 6D and E, it may be that SPCS1 contributes to NS2-E2 complex formation or to stabilizing the complex. Based on data obtained in this study, we propose a model of the formation of an E2-SPCS1-NS2 complex at the ER membrane (Fig. 7).

In summary, we identified SPCS1 as a novel NS2-binding host factor required for HCV assembly by split-ubiquitin membrane yeast two-hybrid screening. Our data demonstrate that SPCS1 plays a key role in the E2-NS2 interaction via formation of an E2-SPCS1-NS2 complex. These findings provide clues for understanding the molecular mechanism of assembly and formation of infectious HCV particles.

## Materials and Methods

### Split ubiquitin-based yeast two-hybrid screen

A split-ubiquitin membrane yeast two-hybrid screen was performed to identify possible NS2 binding partners. This screening system (DUALmembrane system; Dualsystems Biotech, Schlieren, Switzerland) is based on an adaptation of the ubiquitin-based split protein sensor [26]. The full-length HCV NS2 gene derived from the JFH-1 strain [29] was cloned into pBT3-SUC bait vector to obtain bait protein fused to the C-terminal half of ubiquitin (NS2-Cub) along with a transcription factor. Prey proteins generated from a human liver cDNA library (Dualsystems Biotech) were expressed as a fusion to the N-terminal half of ubiquitin (NubG). Complex formation between NS2-Cub and NubG-protein from the library leads to cleavage at the C-terminus of reconstituted ubiquitin by ubiquitin-specific protease(s) with consequent translocation of the transcription factor into the nucleus. Library plasmids were recovered from positive transformants, followed by determining the nucleotide sequences of inserted cDNAs, which were identified using the BLAST algorithm with the GenBank database.

### Cell culture

Human embryonic kidney 293T cells, and human hepatoma Huh-7 cells and its derivative cell lines Huh7.5.1 [43] and Huh7-25 [36], were maintained in Dulbecco's modified Eagle medium supplemented with nonessential amino acids, 100 U of penicillin/ml, 100 μg of streptomycin/ml, and 10% fetal bovine serum (FBS) at 37°C in a 5% $CO_2$ incubator.

### Plasmids

Plasmids pCAGC-NS2/JFH1am and pHHJFH1am were previously described [33]. The plasmid pCAGC-p7/JFHam, having

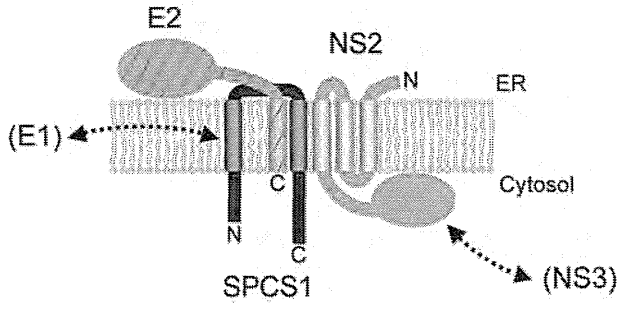


**Figure 7. A proposed model for a complex consisting of NS2, SPCS1 and E2 associated with ER membranes.**
doi:10.1371/journal.ppat.1003589.g007

adaptive mutations in E2 (N417S) and p7 (N765D) in pCAG/C-p7 [44], was constructed by oligonucleotide-directed mutagenesis.

To generate the NS2 expression plasmid pCAG F-NS2 and the NS2-deletion mutants, cDNAs encoding the full-length or parts of NS2 possessing the FLAG-tag and spacer sequences (MDYKDDDDKGGGGS) were amplified from pCAGC-NS2/JFH1am by PCR. The resultant fragments were cloned into pCAGGS. For the NS2-NS3 expression plasmid pEF F-NS2-3, a cDNA encoding the entire NS2 and the N-terminal 226 amino acids of NS3 with the N-terminal FLAG-tag sequence as above was amplified by PCR and was inserted into pEF1/myc-His (Invitrogen, Carlsbad, CA). The plasmid pEF F-NS2-3 H956A, having a defective mutation in the protease active site within NS2, was constructed by oligonucleotide-directed mutagenesis.

To generate the NS3 expression plasmid pCAGN-HANS3JFH1, a cDNA encoding NS3 with an HA tag at the N terminus, which was amplified by PCR with pHHJFHam as a template, was inserted downstream of the CAG promoter of pCAGGS.

To generate the SPCS1-expressing plasmid pCAG-SPCS1-myc and its deletion mutants, cDNAs encoding all of or parts of SPCS1 with the Myc tag sequence (EQKLISEEDL) at the C-terminus, which was amplified by PCR, was inserted into pCAGGS. pSilencer-shSPCS1 carrying a shRNA targeted to SPCS1 under the control of the U6 promoter was constructed by cloning the oligonucleotide pair 5′- GATCCGCAATAGTTGGATTTATCT TTCAAGAGAAGATAAATCCAACTATTGCTTTTTTGGA AA-3′ and 5′- AGCTTTTCCAAAAAAGCAATAGTTGGATT-TATCTTCTCTTGAAAGATAAATCCAACTATTGCG-3′ between the BamHI and HindIII sites of pSilencer 2.1-U6 hygro (Ambion, Austin, TX). To generate a construct expressing shRNA-resistant SPCS1 pSPCS1-sh$^r$, a cDNA fragment coding for SPCS1, in which the 6 bp within the shRNA targeting region (5′-GCAATAGTTGGATTTATCT-3′) was replaced with GCT ATTGTCGGCTTCATAT that causes no aa change, was amplified by PCR. The resulting fragment was confirmed by sequencing and then cloned into pCAGGS.

Full-length SPCS1 and N-terminal region of NS2 (aa 1–94) were amplified by PCR and cloned onto EcoRI and HindIII sites of phmKGN-MN and phmKGC-MN, which encode the mKG fragments (CoralHue Fluo-chase Kit; MBL, Nagoya, Japan), designated as pSPCS1-mKG(N) and pNS2-mKG(C), respectively. Transmembrane domain of the E1 to E2 was also amplified by PCR and cloned onto EcoRI and HindIII sites of phmKGC-MN. To avoid the cleavage of E2-mKG(C) fusion protein in the cells, last alanine of the E2 protein was deleted. Positive control plasmids for mKG system, pCONT-1 and pCONT-2, which encode p65 partial domain from NF-κB complex fused to mKG(N) and p50 partial domain from NF-κB complex fused to mKG(C) respectively, were supplied from MBL. For PLA experiments, cDNA for SPCS1 d2-myc with the V5 tag at the N-terminus was amplified by PCR, and inserted into pCAGGS. For expression of HCV E2, cDNA from E1 signal to the last codon of the transmembrane domain of the E2, in which part of the hypervariable region-1 (aa 394–400) were replaced with FLAG-tag and spacer sequences (DYKDDDDKGGG), was amplified by PCR, and inserted into pCAGGS. For expression of FLAG-core, cDNAs encoding Core (aa 1–152) possessing the FLAG-tag and spacer sequences (MDYKDDDDKGGGGS) were amplified from pCAGC191 [45] by PCR. The resultant fragments were cloned into pCAGGS.

## DNA transfection

Monolayers of 293T cells were transfected with plasmid DNA using FuGENE 6 transfection reagent (Roche, Basel, Switzerland) in accordance with the manufacturer's instructions. Huh-7, Huh7.5.1, and Huh7-25 cells were transfected with plasmid DNA using TransIT LT1 transfection reagent (Mirus, Madison, WI).

## PLA

The assay was performed in a humid chamber at 37°C according to the manufacturer's instructions (Olink Bioscience, Uppsala, Sweden). Transfected 293T cells were grown on glass coverslips. Two days after transfection, cells were fixed with 4% paraformaldehyde in phosphate-buffered saline (PBS) for 20 min, then blocked and permeabilized with 0.3% Triton X-100 in a nonfat milk solution (Block Ace; Snow Brand Milk Products Co., Sapporo, Japan) for 60 min at room temperature. Then the samples were incubated with a mixture of mouse anti-FLAG monoclonal antibody M2 and rabbit anti-V5 polyclonal antibody for 60 min, washed three times, and incubated with plus and minus PLA probes. After washing, the ligation mixture containing connector oligonucleotide was added for 30 min. The washing step was repeated, and amplification mixture containing fluorescently labeled DNA probe was added for 100 min. Finally, the samples were washed and mounted with DAPI mounting medium. The signal representing interaction was analyzed by Leica TCS SPE confocal microscope.

## mKG system

The assay was performed according to the manufacturer's instructions (CoralHue Fluo-chase Kit; MBL). 293T cells were transfected by a pair of mKG fusion constructs. Twenty-four hours after transfection, cell were fixed and stained with DAPI. The signal representing interaction was analyzed by Leica TCS SPE confocal microscope.

## Gene silencing by siRNA

The siRNAs were purchased from Sigma-Aldrich (St. Louis, MO) and were introduced into the cells at a final concentration of 10 to 30 nM using Lipofectamine RNAiMAX (Invitrogen). Target sequences of the siRNAs were as follows: SPCS1 #1 (5′-CAGUUCGGGUGGACUGUCU-3′), SPCS1 #2 (5′-GCAAUA GUUGGAUUUAUCU-3′), SPCS1 #3 (5′-GAUGUUUCAGG-GAAUUAUU-3′), SPCS1 #4 (5′-GUUAUGGCCGGAUUUG-CUU-3′), claudin-1 (5′-CAGUCAAUGCCAGGUACGA-3′), PI4K (5′-GCAAUGUGCUUCGCGAGAA-3′) and scrambled negative control (5′-GCAAGGGAAACCGUGUAAU-3′). Additional control siRNAs for SPCS1 were as follows: C911-#2 (5′-GCAAUAGUaccAUUUAUCU-3′), C911-#3 (5′-GAUGUUU-CuccGAAUUAUU-3′) and C911-#4 (5′-GUUAUGGCgccAUU UGCUU-3′). Bases 9 through 11 of the siRNAs replaced with their complements were shown in lower cases.

## Establishment of a stable cell line expressing the shRNA

Huh-7 cells were transfected with pSilencer-SPCS1, and drug-resistant clones were selected by treatment with hygromycin B (Wako, Tokyo, Japan) at a final concentration of 500 μg/ml for 4 weeks.

## Virus

HCVtcp and HCVcc derived from JFH-1 having adaptive mutations in E2 (N417S), p7 (N765D), and NS2 (Q1012R) were generated as described previously [33]. The rAT strain of JEV [46] was used to generate virus stock.

## Antibodies

Mouse monoclonal antibodies against actin (AC-15) and FLAG (M2) were obtained from Sigma-Aldrich (St. Louis, MO). Mouse

monoclonal antibodies against flavivirus group antigen (D1-4G2) were obtained from Millipore (Billerica, MA). Rabbit polyclonal antibodies against FLAG and V5 were obtained from Sigma-Aldrich. Rabbit polyclonal antibodies against SPCS1, claudin-1, PI4K and myc were obtained from Proteintech (Chicago, IL), Life Technologies (Carlsbad, CA), Cell Signaling (Danvers, MA) and Santa Cruz Biotechnology (Santa Cruz, CA), respectively. An anti-apoE goat polyclonal antibody was obtained from Millipore. Rabbit polyclonal antibodies against NS2 and NS3 were generated with synthetic peptides as antigens. Mouse monoclonal antibodies against HCV Core (2H9) and E2 (8D10-3) and rabbit polyclonal antibodies against NS5A and JEV are described elsewhere [47].

### Titration

To determine the titers of HCVcc, Huh7.5.1 cells in 96-well plates were incubated with serially-diluted virus samples and then replaced with media containing 10% FBS and 0.8% carboxymethyl cellulose. Following incubation for 72 h, the monolayers were fixed and immunostained with the anti-NS5A antibody, followed by an Alexa Fluor 488-conjugated anti-rabbit secondary antibody (Invitrogen). Stained foci were counted and used to calculate the titers of focus-forming units (FFU)/ml. For intracellular infectivity of HCVcc, the pellets of infected cells were resuspended in culture medium and were lysed by four freeze-thaw cycles. After centrifugation for 5 min at 4,000 rpm, supernatants were collected and used for virus titration as above. For titration of JEV, Huh7.5.1 cells were incubated with serially-diluted virus samples and then replaced with media containing 10% FBS and 0.8% carboxymethyl cellulose. After a 24 h incubation, the monolayers were fixed and immunostained with a mouse monoclonal anti-flavivirus group antibody (D1-4G2), followed by an Alexa Fluor 488-conjugated anti-mouse secondary antibody (Invitrogen).

### Immunoprecipitation

Transfected cells were washed with ice-cold PBS, and suspended in lysis buffer (20 mM Tris-HCl [pH 7.4] containing 135 mM NaCl, 1% TritonX-100, and 10% glycerol) supplemented with 50 mM NaF, 5 mM $Na_3VO_4$, and complete protease inhibitor cocktail, EDTA free (Roche). Cell lysates were sonicated for 10 min and then incubated for 30 min at 4°C, followed by centrifugation at 14,000× *g* for 10 min. The supernatants were immunoprecipitated with anti-Myc-agarose beads (sc-40, Santa Cruz Biotechnology) or anti-FLAG antibody in the presence of Dynabeads Protein G (Invitrogen). The immunocomplexes were precipitated with the beads by centrifugation at 800× *g* for 30 s, or by applying a magnetic field, and then were washed four times with the lysis buffer. The proteins binding to the beads were boiled with SDS sample buffer and then subjected to SDS–polyacrylamide gel electrophoresis (PAGE).

### Immunoblotting

Transfected cells were washed with PBS and lysed with 50 mM Tris-HCl, pH 7.4, 300 mM NaCl, 1% Triton X-100. Lysates were then sonicated for 10 min and added to the same volume of SDS sample buffer. The protein samples were boiled for 10 min, separated by SDS-PAGE, and transferred to polyvinylidene difluoride membranes (Millipore). After blocking, the membranes were probed with the primary antibodies, followed by incubation with peroxidase-conjugated secondary antibody. Antigen-antibody complexes were visualized by an enhanced chemiluminescence detection system (Super Signal West Pico Chemiluminescent Substrate; PIERCE, Rockford, IL) according to the manufacturer's protocol and were detected by an LAS-3000 image analyzer system (Fujifilm, Tokyo, Japan).

### Albumin measurement

To determine the human albumin level secreted from cells, culture supernatants were collected and passed through a 0.45-μm pore filter to remove cellular debris. The amounts of human albumin were quantified using a human albumin ELISA kit (Bethyl Laboratories, Montgomery, TX) according to the manufacturer's protocol.

## Supporting Information

**Figure S1** Effects of SPCS1-siRNAs and the C911 mismatch control siRNAs on the expression of SPCS1 and production of HCV. (A) Huh7.5.1 cells were transfected with either siRNAs targeted for SPCS1 (SPCS1-#2, -#3, and -#4), scrambled control siRNA (Scrambled) or C911 siRNA in which bases 9 through 11 of each SPCS1 siRNA were replaced with their complements (C911-#2, -#3, and -#4) at a final concentration of 15 nM, and were infected with HCVcc at a multiplicity of infection (MOI) of 0.05 at 24 h post-transfection. Expression levels of endogenous SPCS1 and actin in the cells were examined by immunoblotting using anti-SPCS1 and anti-actin antibodies at 3 days post-infection. (B) Infectious titers of HCVcc in the supernatant of the infected cells were determined at 3 days postinfection.
(TIF)

**Figure S2** 293T cells were transfected with E2 expression plasmid in the presence or absence of SPCS1-myc expression plasmid. The cell lysates of the transfected cells were immunoprecipitated with anti-myc antibody. The resulting precipitates and whole cell lysates used in IP were examined by immunoblotting using anti-E2 or anti-myc antibody. An empty plasmid was used as a negative control.
(TIF)

**Figure S3** Interaction of HCV E2 with SPCS1 in mammalian cells. (A) 293T cells were transfected with indicated plasmids. 2 days posttransfection, cells were fixed and permeabilized with Triton X-100, then subjected to in situ PLA (Upper) or immunofluorescence staining (Lower) using anti-FLAG and anti-V5 antibodies. (B) Detection of the SPCS1-E2 interaction in transfected cells using the mKG system. 293T cells were transfected by indicated pair of mKG fusion constructs. Twenty-four hours after transfection, cell were fixed and stained with DAPI, and observed under a confocal microscope.
(TIF)

## Acknowledgments

We are grateful to Francis V. Chisari (The Scripps Research Institute) for providing Huh7.5.1 cells, and Drs. C.K. Lim and T. Takasaki (National Institute of Infectious Diseases) for providing rabbit polyclonal anti-JEV antibodies. We thank M. Sasaki and T. Date for their technical assistance, and T. Mizoguchi for secretarial work. We also thank H. Hasegawa, T. Kato, T. Masaki, N. Watanabe, and A. Murayama for their helpful discussions.

## Author Contributions

Conceived and designed the experiments: RS TS. Performed the experiments: RS MM. Analyzed the data: RS KW HA TS. Contributed reagents/materials/analysis tools: YM TW. Wrote the paper: RS TS.

## References


1. Hoofnagle JH (2002) Course and outcome of hepatitis C. Hepatology 36: S21–29.
2. Suzuki T, Aizaki H, Murakami K, Shoji I, Wakita T (2007) Molecular biology of hepatitis C virus. J Gastroenterol 42: 411–423.
3. Appel N, Zayas M, Miller S, Krijnse-Locker J, Schaller T, et al. (2008) Essential role of domain III of nonstructural protein 5A for hepatitis C virus infectious particle assembly. PLoS Pathog 4: e1000035.
4. Dentzer TG, Lorenz IC, Evans MJ, Rice CM (2009) Determinants of the hepatitis C virus nonstructural protein 2 protease domain required for production of infectious virus. J Virol 83: 12702–12713.
5. Jirasko V, Montserret R, Appel N, Janvier A, Eustachi L, et al. (2008) Structural and functional characterization of nonstructural protein 2 for its role in hepatitis C virus assembly. J Biol Chem 283: 28546–28562.
6. Jones CT, Murray CL, Eastman DK, Tassello J, Rice CM (2007) Hepatitis C virus p7 and NS2 proteins are essential for production of infectious virus. J Virol 81: 8374–8383.
7. Ma Y, Yates J, Liang Y, Lemon SM, Yi M (2008) NS3 helicase domains involved in infectious intracellular hepatitis C virus particle assembly. J Virol 82: 7624–7639.
8. Masaki T, Suzuki R, Murakami K, Aizaki H, Ishii K, et al. (2008) Interaction of hepatitis C virus nonstructural protein 5A with core protein is critical for the production of infectious virus particles. J Virol 82: 7964–7976.
9. Tellinghuisen TL, Foss KL, Treadaway J (2008) Regulation of hepatitis C virion production via phosphorylation of the NS5A protein. PLoS Pathog 4: e1000032.
10. Phan T, Beran RK, Peters C, Lorenz IC, Lindenbach BD (2009) Hepatitis C virus NS2 protein contributes to virus particle assembly via opposing epistatic interactions with the E1–E2 glycoprotein and NS3-NS4A enzyme complexes. J Virol 83: 8379–8395.
11. Lorenz IC, Marcotrigiano J, Dentzer TG, Rice CM (2006) Structure of the catalytic domain of the hepatitis C virus NS2-3 protease. Nature 442: 831–835.
12. Lohmann V, Korner F, Koch J, Herian U, Theilmann L, et al. (1999) Replication of subgenomic hepatitis C virus RNAs in a hepatoma cell line. Science 285: 110–113.
13. Kato T, Choi Y, Elmowalid G, Sapp RK, Barth H, et al. (2008) Hepatitis C virus JFH-1 strain infection in chimpanzees is associated with low pathogenicity and emergence of an adaptive mutation. Hepatology 48: 732–740.
14. Scheel TK, Gottwein JM, Jensen TB, Prentoe JC, Hoegh AM, et al. (2008) Development of JFH1-based cell culture systems for hepatitis C virus genotype 4a and evidence for cross-genotype neutralization. Proc Natl Acad Sci U S A 105: 997–1002.
15. Jensen TB, Gottwein JM, Scheel TK, Hoegh AM, Eugen-Olsen J, et al. (2008) Highly efficient JFH1-based cell-culture system for hepatitis C virus genotype 5a: failure of homologous neutralizing-antibody treatment to control infection. J Infect Dis 198: 1756–1765.
16. Yi M, Ma Y, Yates J, Lemon SM (2007) Compensatory mutations in E1, p7, NS2, and NS3 enhance yields of cell culture-infectious intergenotypic chimeric hepatitis C virus. J Virol 81: 629–638.
17. Russell RS, Meunier JC, Takikawa S, Faulk K, Engle RE, et al. (2008) Advantages of a single-cycle production assay to study cell culture-adaptive mutations of hepatitis C virus. Proc Natl Acad Sci U S A 105: 4370–4375.
18. Popescu CI, Callens N, Trinel D, Roingeard P, Moradpour D, et al. (2011) NS2 protein of hepatitis C virus interacts with structural and non-structural proteins towards virus assembly. PLoS Pathog 7: e1001278.
19. Ma Y, Anantpadma M, Timpe JM, Shanmugam S, Singh SM, et al. (2011) Hepatitis C virus NS2 protein serves as a scaffold for virus assembly by interacting with both structural and nonstructural proteins. J Virol 85: 86–97.
20. Stapleford KA, Lindenbach BD (2011) Hepatitis C virus NS2 coordinates virus particle assembly through physical interactions with the E1–E2 glycoprotein and NS3-NS4A enzyme complexes. J Virol 85: 1706–1717.
21. Jirasko V, Montserret R, Lee JY, Gouttenoire J, Moradpour D, et al. (2010) Structural and functional studies of nonstructural protein 2 of the hepatitis C virus reveal its key role as organizer of virion assembly. PLoS Pathog 6: e1001233.
22. Yi M, Ma Y, Yates J, Lemon SM (2009) Trans-complementation of an NS2 defect in a late step in hepatitis C virus (HCV) particle assembly and maturation. PLoS Pathog 5: e1000403.
23. Counihan NA, Rawlinson SM, Lindenbach BD (2011) Trafficking of hepatitis C virus core protein during virus particle assembly. PLoS Pathog 7: e1002302.
24. Kiiver K, Merits A, Ustav M, Zusinaite E (2006) Complex formation between hepatitis C virus NS2 and NS3 proteins. Virus Res 117: 264–272.
25. Selby MJ, Glazer E, Masiarz F, Houghton M (1994) Complex processing and protein:protein interactions in the E2:NS2 region of HCV. Virology 204: 114–122.
26. Johnsson N, Varshavsky A (1994) Split ubiquitin as a sensor of protein interactions in vivo. Proc Natl Acad Sci U S A 91: 10340–10344.
27. Evans E, A., Gilmore R, Blobel G (1986) Purification of microsomal signal peptidase as a complex. Proc Natl Acad Sci U S A 83: 581–585.
28. Fang H, Panzner S, Mullins C, Hartmann E, Green N (1996) The homologue of mammalian SPC12 is important for efficient signal peptidase activity in Saccharomyces cerevisiae. J Biol Chem 271: 16460–16465.
29. Wakita T, Pietschmann T, Kato T, Date T, Miyamoto M, et al. (2005) Production of infectious hepatitis C virus in tissue culture from a cloned viral genome. Nat Med 11: 791–796.
30. Söderberg O, Gullberg M, Jarvius M, Ridderstrale K, Leuchowius KJ, et al. (2006) Direct observation of individual endogenous protein complexes in situ by proximity ligation. Nat Methods 3: 995–1000.
31. Kerppola TK (2006) Complementary methods for studies of protein interactions in living cells. Nat Methods 3: 969–971.
32. Buehler E, Chen YC, Martin S (2012) C911: A bench-level control for sequence specific siRNA off-target effects. PLoS One 7: e51942.
33. Suzuki R, Saito K, Kato T, Shirakura M, Akazawa D, et al. (2012) Trans-complemented hepatitis C virus particles as a versatile tool for study of virus assembly and infection. Virology 432: 29–38.
34. Chang KS, Jiang J, Cai Z, Luo G (2007) Human apolipoprotein E is required for infectivity and production of hepatitis C virus in cell culture. J Virol 81: 13783–13793.
35. Owen DM, Huang H, Ye J, Gale M, Jr. (2009) Apolipoprotein E on hepatitis C virion facilitates infection through interaction with low-density lipoprotein receptor. Virology 394: 99–108.
36. Akazawa D, Date T, Morikawa K, Murayama A, Miyamoto M, et al. (2007) CD81 expression is important for the permissiveness of Huh7 cell clones for heterogeneous hepatitis C virus infection. J Virol 81: 5036–5045.
37. Erdtmann L, Franck N, Lerat H, Le Seyec J, Gilot D, et al. (2003) The hepatitis C virus NS2 protein is an inhibitor of CIDE-B-induced apoptosis. J Biol Chem 278: 18256–18264.
38. de Chassey B, Navratil V, Tafforeau L, Hiet MS, Aublin-Gex A, et al. (2008) Hepatitis C virus infection protein network. Mol Syst Biol 4: 230.
39. Stagljar I, Korostensky C, Johnsson N, te Heesen S (1998) A genetic system based on split-ubiquitin for the analysis of interactions between membrane proteins in vivo. Proc Natl Acad Sci U S A 95: 5187–5192.
40. Kalies KU, Hartmann E (1996) Membrane topology of the 12- and the 25-kDa subunits of the mammalian signal peptidase complex. J Biol Chem 271: 3925–3929.
41. Mullins C, Meyer HA, Hartmann E, Green N, Fang H (1996) Structurally related Spc1p and Spc2p of yeast signal peptidase complex are functionally distinct. J Biol Chem 271: 29094–29099.
42. Li Q, Brass AL, Ng A, Hu Z, Xavier RJ, et al. (2009) A genome-wide genetic screen for host factors required for hepatitis C virus propagation. Proc Natl Acad Sci U S A 106: 16410–16415.
43. Zhong J, Gastaminza P, Cheng G, Kapadia S, Kato T, et al. (2005) Robust hepatitis C virus infection in vitro. Proc Natl Acad Sci U S A 102: 9294–9299.
44. Masaki T, Suzuki R, Saeed M, Mori K, Matsuda M, et al. (2010) Production of infectious hepatitis C virus by using RNA polymerase I-mediated transcription. J Virol 84: 5824–5835.
45. Suzuki R, Sakamoto S, Tsutsumi T, Rikimaru A, Tanaka K, et al. (2005) Molecular determinants for subcellular localization of hepatitis C virus core protein. J Virol 79: 1271–1281.
46. Zhao Z, Date T, Li Y, Kato T, Miyamoto M, et al. (2005) Characterization of the E-138 (Glu/Lys) mutation in Japanese encephalitis virus by using a stable, full-length, infectious cDNA clone. J Gen Virol 86: 2209–2220.
47. Saeed M, Suzuki R, Watanabe N, Masaki T, Tomonaga M, et al. (2011) Role of the endoplasmic reticulum-associated degradation (ERAD) pathway in degradation of hepatitis C virus envelope proteins and production of virus particles. J Biol Chem 286: 37264–37273.

Biochemical and Biophysical Research Communications 440 (2013) 515–520

Contents lists available at ScienceDirect

Biochemical and Biophysical Research Communications

journal homepage: www.elsevier.com/locate/ybbrc

# Specific inhibition of hepatitis C virus entry into host hepatocytes by fungi-derived sulochrin and its derivatives

Syo Nakajima [a,b], Koichi Watashi [a,b,*], Shinji Kamisuki [b], Senko Tsukuda [a,c], Kenji Takemoto [b], Mami Matsuda [a], Ryosuke Suzuki [a], Hideki Aizaki [a], Fumio Sugawara [b], Takaji Wakita [a]

[a] Department of Virology II, National Institute of Infectious Diseases, Tokyo 162-8640, Japan
[b] Tokyo University of Science Graduate School of Science and Technology, Noda 278-8510, Japan
[c] Micro-Signaling Regulation Technology Unit, RIKEN Center for Life Science Technologies, Wako 351-0198, Japan

ARTICLE INFO

*Article history:*
Received 5 September 2013
Available online 5 October 2013

*Keywords:*
HCV
Entry
Sulochrin
Natural product
Screening
Compound

ABSTRACT

Hepatitis C virus (HCV) is a major causative agent of hepatocellular carcinoma. Although various classes of anti-HCV agents have been under clinical development, most of these agents target RNA replication in the HCV life cycle. To achieve a more effective multidrug treatment, the development of new, less expensive anti-HCV agents that target a different step in the HCV life cycle is needed. We prepared an in-house natural product library consisting of compounds derived from fungal strains isolated from seaweeds, mosses, and other plants. A cell-based functional screening of the library identified sulochrin as a compound that decreased HCV infectivity in a multi-round HCV infection assay. Sulochrin inhibited HCV infection in a dose-dependent manner without any apparent cytotoxicity up to 50 μM. HCV pseudoparticle and trans-complemented particle assays suggested that this compound inhibited the entry step in the HCV life cycle. Sulochrin showed anti-HCV activities to multiple HCV genotypes 1a, 1b, and 2a. Co-treatment of sulochrin with interferon or a protease inhibitor telaprevir synergistically augmented their anti-HCV effects. Derivative analysis revealed anti-HCV compounds with higher potencies ($IC_{50}$ < 5 μM). This is the first report showing an antiviral activity of methoxybenzoate derivatives. Thus, sulochrin derivatives are anti-HCV lead compounds with a new mode of action.



## 1. Introduction

Hepatitis C virus (HCV) infection is a major causative agent of chronic liver diseases such as liver cirrhosis and hepatocellular carcinoma [1]. The standard anti-HCV therapy has been a co-treatment with pegylated-interferon (IFN)α and ribavirin, but this therapy is limited by less efficacy to certain HCV genotypes, poor tolerability, serious side effects, and high cost [2,3]. In addition to the newly approved protease inhibitors, telaprevir and boceprevir, a variety of anti-HCV candidates are under clinical development. Although these drugs improve the virological response rate, the emergence of drug-resistant virus is expected to be a significant problem. Moreover, these compounds are expensive due to their complex structure and the many steps required for their total synthesis. To overcome the drug-resistant virus and achieve a long-term antiviral effect, multidrug treatment is essential. Thus, the development of drugs targeting a different step in the HCV life cycle and presumably requiring low cost is urgently needed.

HCV propagates in hepatocytes through its viral life cycle including: attachment and entry (defined as the early step in this study); translation, polyprotein processing, and RNA replication (the middle step); and assembly, trafficking, budding, and release (the late step) (Supplementary Fig. S1). The middle step has been extensively analysed, especially after the establishment of the HCV replicon system [4]. The early step can be analysed with HCV pseudoparticle (HCVpp) [5,6], which is a murine leukemia virus- or human immunodeficiency virus-based pseudovirus carrying HCV E1 and E2 as envelope proteins. The HCV-producing cell culture system (HCVcc) is used for analyzing the whole life cycle [7–9]. In addition, the HCV trans-complemented particle (HCVtcp) system carrying an HCV subgenomic replicon RNA packaged in HCV E1 and E2-containing particles can evaluate the life cycle from the early to the middle step [10]. The majority of anti-HCV agents currently under clinical development, such as inhibitors of protease, polymerase, NS5A, and cellular cyclophilin, inhibit polyprotein processing and/or RNA replication. A desirable approach

*Abbreviations:* HCV, hepatitis C virus; IFN, interferon; HCVpp, HCV pseudoparticle; HCVcc, HCV derived from cell culture; HCVtcp, HCV trans-complemented particle; MOI, multiplicity of infection; HBs, HBV envelope protein; CsA, cyclosporin A; VSV, vesicular stomatitis virus.

* Corresponding author. Adress: Department of Virology II, National Institute of Infectious Diseases, 1-23-1 Toyama, Shinjuku-ku, Tokyo 162-8640, Japan. Fax: +81 3 5285 1161.
*E-mail address:* kwatashi@nih.go.jp (K. Watashi).

0006-291X/$ - see front matter © 2013 Elsevier Inc. All rights reserved.
http://dx.doi.org/10.1016/j.bbrc.2013.09.100

to achieving efficient multidrug therapy is to identify new antiviral drugs targeting different steps in the viral life cycle. A combination of drugs with different targets can greatly decrease the emergence of drug-resistant virus.

Natural products generally contain more characteristics of high chemical diversity than combinatorial chemical collections, and therefore have a wider range of physiological activities [11,12]. They offer major opportunities for finding novel lead structures that are active in a biological assay. Moreover, biologically active natural products are generally small molecules with drug-like properties, and thus development costs of producing orally active agents tend to be lower than that derived from combinatorial chemistry [13]. In addition, there is a wide variety of natural compounds reported to possess antiviral activity [14,15]. In the present study, we have taken advantage of the potential of natural products by screening a natural product library derived from fungal extracts with a cell-based assay that supports the whole life cycle of HCV.

## 2. Materials and methods

### 2.1. Cell culture

Huh-7.5.1 [8] and HepaRG cells [16] were cultured as described previously.

### 2.2. Natural product library and reagents

Natural products were extracted essentially as previously described [17]. Culture broths of fungal strains isolated from seaweeds, mosses, and other plants were extracted with $CH_2Cl_2$. The crude extracts were separated by silica gel column chromatography to purify compounds. The chemical structure of each compound was determined by NMR and mass spectrometry analyses. Thus, we prepared an in-house natural product library consisting of approximately 300 isolated compounds.

Cyclosporin A was purchased from Sigma. Bafilomycin A1 and chlorpromazine were purchased from Wako. Heparin was obtained from Mochida Pharmaceutical. IFNα was purchased from Schering-Plough.

### 2.3. Compound screening

Huh-7.5.1 cells were treated with HCV J6/JFH1 at a multiplicity of infection (MOI) of 0.15 for 4 h. The cells were washed and then cultured with growth medium treated with 10 μM of each compound for 72 h. The infectivity of HCV in the medium was quantified. Cell viability at 72 h post-treatment was simultaneously measured. Compounds that decreased the cell viability to less than 50% of that without treatment were eliminated for further evaluations. Normalised infectivity was calculated as HCV infectivity divided by cell viability. Compounds reducing the normalised infectivity to less than 40% were selected as initial hits. The initial hits were further evaluated for data reproduction and dose-dependency.

### 2.4. HCVcc assay

HCVcc was recovered from the medium of Huh-7.5.1 cells transfected with HCV J6/JFH-1 RNA as described [7]. HCVcc was infected into Huh-7.5.1 cells at 0.15 MOI for 4 h. After washing out the inoculated virus, the cells were cultured with normal growth medium in the presence or absence of compounds for 72 h. The infectivity of HCV and the amount of HCV core protein in the medium were quantified by infectious focus formation assay and chemiluminescent enzyme immunoassay (Lumipulse II HCV core assay, ortho clinical diagnostics), respectively [7,18].

### 2.5. Immunoblot analysis

Immunoblot analysis was performed as described previously [19]. The anti-HCV core antibody (2H9) was used as a primary antibody with 1:1000 dilution [7].

### 2.6. MTT assay

The viability of cells was quantified by using a Cell Proliferation Kit II XTT (Roche Diagnostics) as described previously [20].

### 2.7. HCV replicon assay

Huh-7.5.1 cells were transfected with an HCV subgenome replicon RNA (SGR-JFH1/Luc) for 4 h and then incubated with or without compounds for 48 h [21]. The cells were lysed with 1xPLB (Promega), and the luciferase activity was determined with a luciferase assay system (Promega) according to the manufacturer's protocol [22].

### 2.8. HCVpp assay

HCVpp was recovered from the medium of 293T cells transfected with expression plasmids for HCV JFH-1 E1E2, MLV Gag-Pol, and luciferase, which were kindly provided from Dr. Francois-Loic Cosset at Universite de Lyon [5]. Vesicular stomatitis virus pseudoparticles (VSVpp) was similarly recovered with transfection by replacing HCV E1E2 with VSV G.

Huh-7.5.1 cells were preincubated with compounds for 3 h and were then infected with HCVpp in the presence of compounds for 4 h. After washing out virus and compounds, cells were incubated for an additional 72 h before recovering the cell lysates and quantifying the luciferase activity.

### 2.9. HCVtcp assay

The HCVtcp assay was essentially performed as described [10]. Briefly, Huh-7 cells were transfected with expression plasmids for the HCV subgenomic replicon carrying the luciferase gene and for HCV core-NS2 based on genotype 1a (RMT) (kindly provided by Dr. Michinori Kohara at Tokyo Metropolitan Institute of Medical Science), 1b (Con1), and 2a (JFH-1) [4,10,23] to recover HCVtcp. HCVtcp can reproduce RNA replication as well as HCV-mediated entry into the cells [10].

### 2.10. Synergy analysis

To determine whether the effect of the drug combination was synergistic, additive, or antagonistic, MacSynergy (kindly provided by Mark Prichard), a mathematical model based on the Bliss independence theory, was used to analyse the experimental data shown in Fig. 3A. In this model, a theoretical additive effect with any given concentrations can be calculated by $Z = X + Y(1-X)$, where $X$ and $Y$ represent the inhibition produced by each drug alone, and $Z$ represents the effect produced by the combination of two compounds if they were additive. The theoretical additive effects were compared to the actual experimental effects at various concentrations of the two compounds and were plotted as a three-dimensional differential surface that would appear as a horizontal plane at 0 if the combination were additive. Any peak above this plane (positive values) indicates synergy, whereas any depression below the plane (negative values) indicates antagonism. The 95% confidence interval of the experimental dose–response was considered to reveal only effects that were statistically significant.

## 3. Results

### 3.1. Screening of natural products possessing anti-HCV activity

We extracted culture broths of fungal strains isolated from seaweeds, mosses, and other plants and purified compounds as described in the Section 2 [17]. The chemical structure of each compound was determined by NMR and mass spectrometry analyses. Thus, we prepared an in-house natural product library consisting of approximately 300 isolated compounds. As shown in the Section 2, compounds reducing the normalised HCV infectivity to less than 40% as compared with DMSO were selected as primary hits. The primary hits were then validated by examining the reproducibility, dose-dependency, and cell viability in the HCVcc system. Sulochrin [methyl 2-(2,6-dihydroxy-4-methylbenzoyl)-5-hydroxy-3-methoxybenzoate] (Fig. 1A) was one of the compounds showing the highest anti-HCV activity, and the following analyses focus mainly on this compound.

### 3.2. Sulochrin decreased HCV infectivity in HCV cell culture assay

To characterise the anti-HCV activity of the compounds, Huh-7.5.1 cells were infected with HCV J6/JFH1 at an MOI of 0.15 and then cultured for 72 h in the presence or absence of compounds.

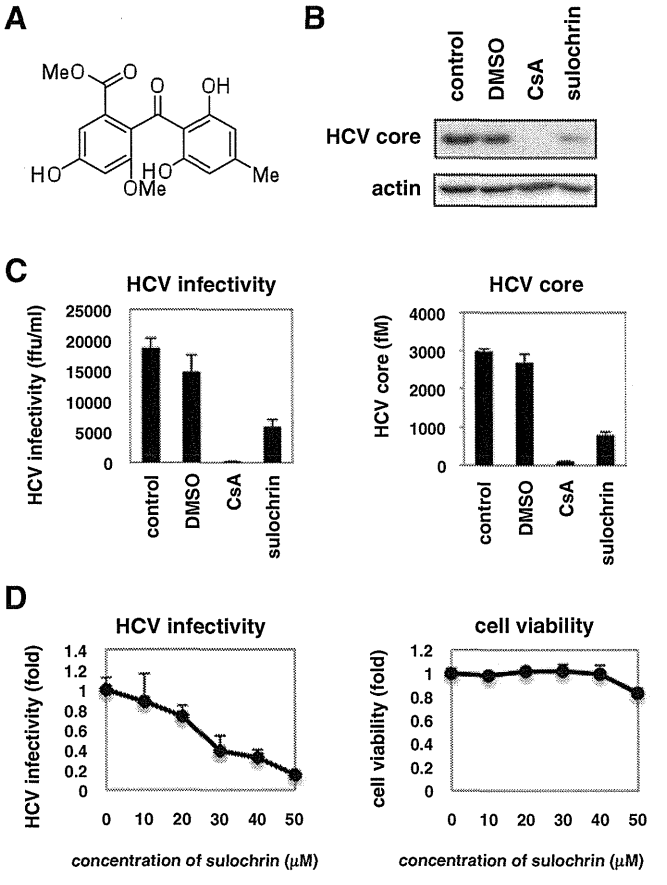


**Fig. 1.** Sulochrin decreased HCV production in a multi-round HCV infection assay. (A) Chemical structure of sulochrin. (B) Huh-7.5.1 cells were infected with HCV J6/JFH-1 at an MOI of 0.15 for 4 h and then incubated with or without 0.3% DMSO, 2 μM cyclosporin A (CsA), or 30 μM sulochrin for 72 h. The resultant medium was inoculated into naïve Huh-7.5.1 cells to detect intracellular HCV core and actin protein at 48 h postinoculation by immunoblot. (C) HCV infectivity (left) and HCV core protein (right) in the medium as prepared in (B) were quantified as shown in the Section 2. (D) HCV infectivity (left) determined as shown in (C) with varying concentrations (0–50 μM) of sulochrin. Cell viability was examined by MTT assay (right).

In this system, infectious HCV is secreted into the medium and then re-infects into uninfected cells to support the spread of HCV during a 72 h period (Section 2). Cell cultures were treated with sulochrin or cyclosporin A (CsA) as a positive control in this mul-

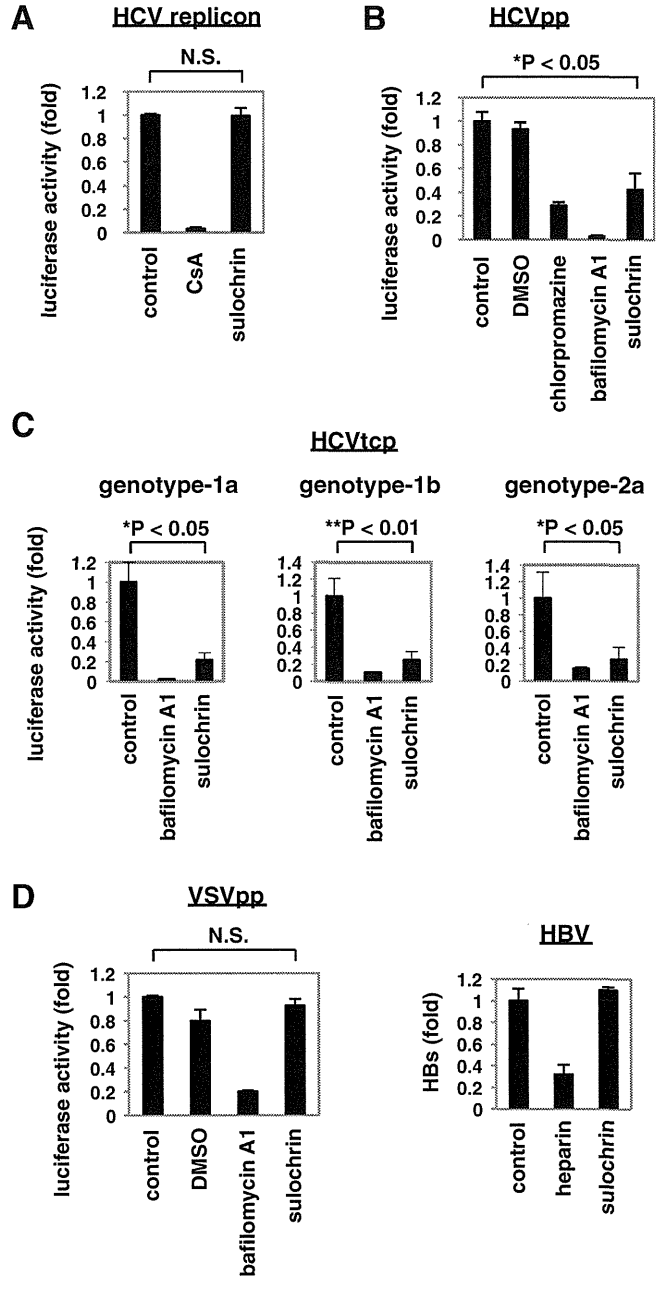


**Fig. 2.** Sulochrin blocked HCV entry. (A) Replicon assay. Huh-7.5.1 cells were transfected with an HCV subgenomic replicon RNA for 4 h followed by treatment with or without the indicated compounds for 48 h. Luciferase activity driven by the replication of the subgenomic replicon was quantified. (B and C) HCV pseudoparticle (HCVpp) and trans-complemented particle (HCVtcp) assay. Huh-7.5.1 cells were pretreated with the indicated compounds for 3 h and then infected with HCVpp (B) or HCVtcp (C) for 4 h. After washing out virus and compounds, cells were further incubated for 72 h and harvested for measuring luciferase activity driven by the infection of HCVpp or HCVtcp. HCVtcp assay was performed with HCV E1 and E2 derived from genotypes 1a (RMT), 1b (Con1), and 2a (JFH1). (D) Left, the pseudoparticle assay was performed as shown in (B) with VSV G instead of HCV E1 and E2. Right, HBV infection assay. HepaRG cells were pretreated with the indicated compounds for 3 h and then infected with HBV for 16 h. After washing out virus and compounds, cells were incubated for an additional 12 days. HBV infection was evaluated by measuring HBs secretion from the infected cells. Heparin was used as a positive control that inhibits HBV entry.

ti-round infection system. To examine the level of infectious HCV particles produced from the cells, the resultant medium was inoculated into naive Huh-7.5.1 cells to detect HCV core protein in the cells. As shown in Fig. 1B, intracellular production of HCV core but not that of actin was reduced in the cells inoculated with sulochrin- and CsA-treated medium (Fig. 1B). Quantitative analysis showed that sulochrin decreased HCV infectivity and HCV core protein in the medium to 1/3–1/4 of the untreated levels (Fig. 1C). Reduction of HCV infectivity by sulochrin was dose-dependent without serious cytotoxicity up to 50 μM (Fig. 1D).

### 3.3. Sulochrin blocked HCV entry

We investigated the step in the HCV life cycle that was inhibited by sulochrin. The middle step of the life cycle including translation and RNA replication was evaluated with the transient replication assay by using the HCV subgenomic replicon. Sulochrin had little effect on the replicon activity at doses up to 50 μM (Fig. 2A). In the HCVpp system, which reproduced the early step of HCV infection including entry, sulochrin significantly inhibited HCVpp infection (Fig. 2B). Sulochrin also inhibited the infection of HCVtcp, which reproduced both the viral entry and RNA replication, further supporting that this compound targeted the entry step (Fig. 2C). In contrast, VSV G-mediated viral entry efficiency was not altered by sulochrin treatment (Fig. 2D). Additionally, HBV entry was not inhibited by the presence of sulochrin (Fig. 2D). These data suggest that the inhibitory activity of sulochrin on viral entry is specific to HCV. The anti-HCV entry activity of sulochrin was conserved among different HCV genotypes, 1a (RMT), 1b (Con1), and 2a (JFH-1) [4,10,23] (Fig. 2C).

### 3.4. Synergistic effect of cotreatment of sulochrin with IFNα or telaprevir

We examined the anti-HCV activity of sulochrin co-administered with clinically available anti-HCV agents, IFNα and a prote-

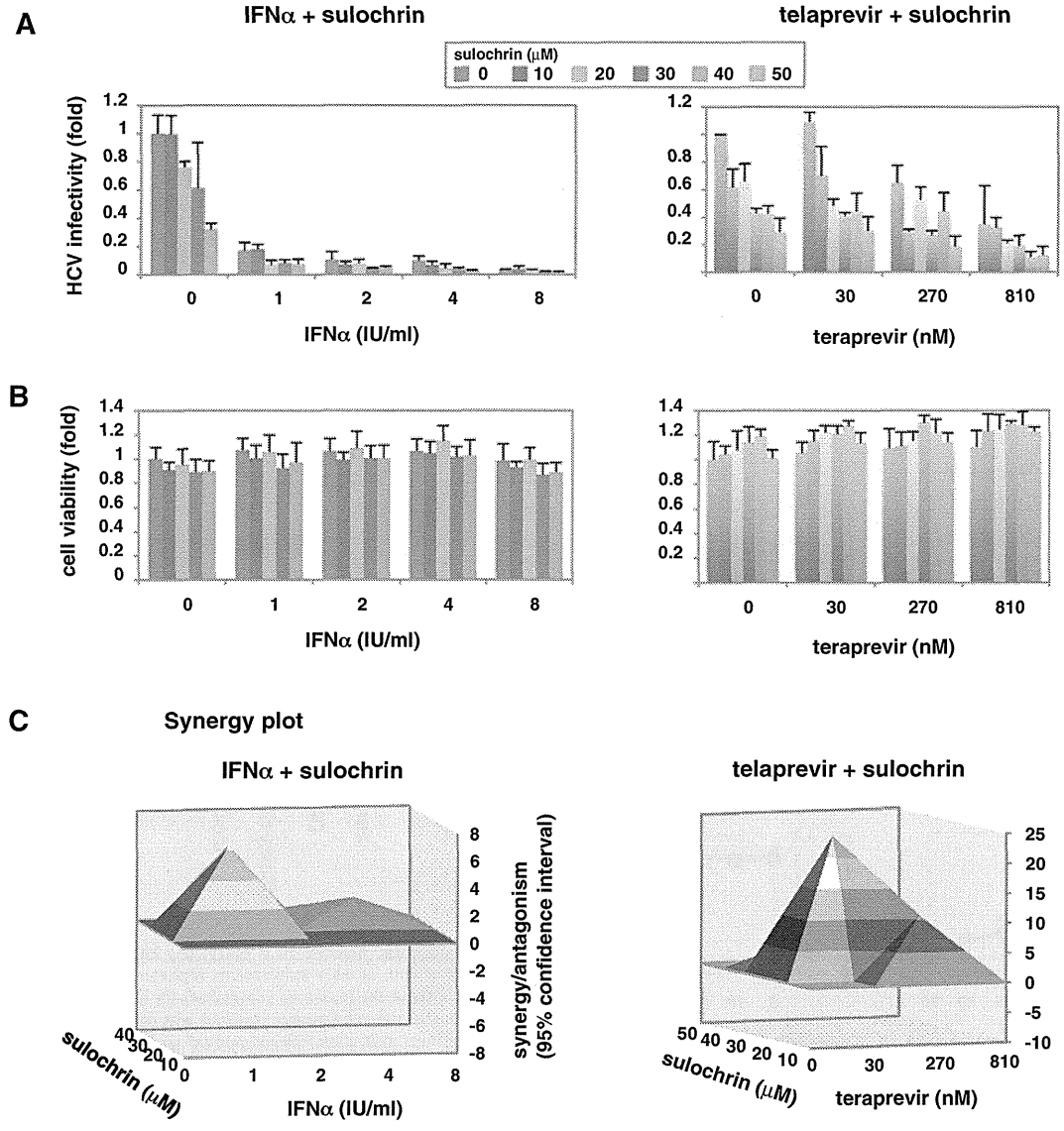


**Fig. 3.** Cotreatment of sulochrin with IFNα or telaprevir. (A, B) Huh-7.5.1 cells infected with HCV were treated with the indicated concentrations of sulochrin with IFNα (left) or telaprevir (right) to determine HCV infectivity in the medium (A) as shown in Fig. 1C. Cell viability was also quantified (B). (C) Synergy analysis. The results of the combinations shown in (A) were analysed with a mathematical model, MacSynergy, as described in the Section 2. The three-dimensional surface plot represents the difference between actual experimental effects and theoretical additive effects of the combination treatment (95% confidence interval). The theoretical additive effects are shown as the zero plane (dark gray) across the *z*-axis. A positive value in the *z*-axis as a peak above the plane indicates synergy, and a negative value with a valley below the plane indicates antagonism. Sulochrin in combination with IFNα (left) or telaprevir (right) produced synergistic antiviral effects that were greater than the theoretical additive effects.

ase inhibitor telaprevir. As shown in Fig. 3, addition of sulochrin with IFNα or telaprevir led to a further decrease in HCV infectivity (Fig. 3A) without significantly enhancing cytotoxicity (Fig. 3B) at any given concentrations. Thus, the combination of sulochrin and IFNα or telaprevir always resulted in a greater reduction in HCV infectivity as compared with that achieved by either agent alone. Synergy/antagonism analysis with the Bliss independence model showed that the experimental anti-HCV activity in combination with sulochrin and IFNα or telaprevir showed a peak above the zero plane in the *z*-axis, which shows the calculated theoretical additive effect (Fig. 3C). Any peak above the zero plane indicates more than an additive effect, namely, synergy (Section 2). The data clearly indicate that sulochrin had a synergistic anti-HCV effect with both IFNα and telaprevir.

### 3.5. Derivative analysis of sulochrin

We examined the anti-HCV activity of a series of sulochrin derivatives (Fig. 4A) in the HCVcc system. Monochlorosulochrin and dihydrogeodin, mono- or dichloro-substituted derivatives of sulochrin, possessed even higher anti-HCV activity than sulochrin (Fig. 4B and C). Deoxyfunicone, of which one aromatic ring was replaced by a 4-pyrone ring, had approximately 5-fold greater HCV inhibitory activity as compared with sulochrin (Fig. 4B and C). An additional compound, 3-*O*-methylfunicone, also possessed anti-HCV activity (Fig. 4B and C). These data suggest that the 1,3-dihydroxy-5-methylbenzene moiety of sulochrin is important for anti-HCV activity. Furthermore, funicone derivatives as well as sulochrin derivatives are likely to be lead compounds for a new class of anti-HCV agents.

## 4. Discussion

In the present study, we prepared a natural product library consisting of approximately 300 isolated compounds derived from fungi extract [17]. Among these compounds, we focused on sulochrin, which reduced HCV infectivity in the HCVcc system. Sulochrin suppressed the viral entry efficiencies both in the HCVpp and the HCVtcp systems, suggesting that this compound blocked HCV envelope-mediated entry. HCV was reported to enter host cells through clathrin-dependent endocytosis after engagement to host receptors [24–27]. Sulochrin is not likely to be a general inhibitor of clathrin-dependent endocytosis, but rather is specific for HCV entry, as it did not affect the entry of other viruses such as VSVpp and HBV, which were reported to enter by clathrin-dependent manners [28,29].

Sulochrin inhibits eosinophil degranulation, activation, and chemotaxis [30,31]. It also inhibits VEGF-induced tube formation of human umbilical vein endothelial cells [32]. In addition, 3-*O*-methylfunicone, a sulochrin derivative possessing anti-HCV activity, has an anti-tumor activity [33]. It is unknown if these activities of the compounds are related to their anti-HCV activity. The establishment of drug-resistant virus and the identification of the target molecule are in progress to reveal the mechanism of action of sulochrin and its derivatives. However, the present study is the

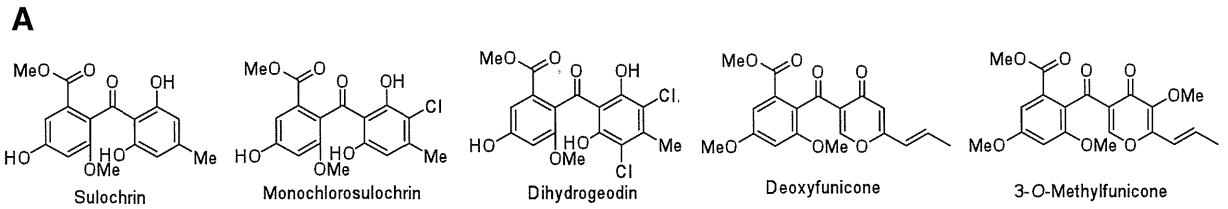


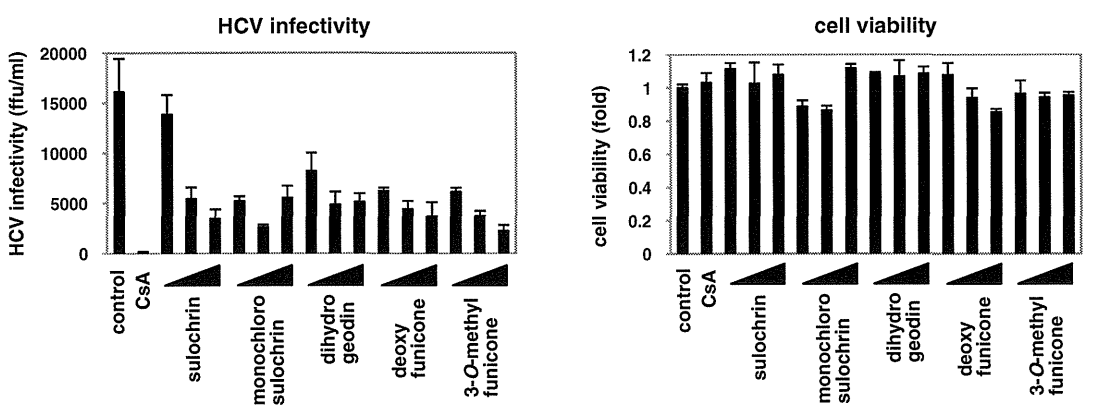


C

$IC_{50}$s and $CC_{50}$s

| compound | $IC_{50}$ (μM) | $CC_{50}$ (μM) |
|---|---|---|
| sulochrin | 24.4 ± 2.0 | > 50 |
| monochlorosulochrin | 4.3 ± 1.1 | > 50 |
| dihydrogeodin | 10.3 ± 0.3 | > 50 |
| deoxyfunicone | 4.6 ± 1.1 | > 50 |
| 3-*O*-methylfunicone | 6.2 ± 2.3 | > 50 |

**Fig. 4.** Derivative analysis of sulochrin. (A) Chemical structures of sulochrin derivatives examined in this study, monochlorosulochrin, dihydrogeodin, deoxyfunicone, 3-*O*-methyfunicone, as well as sulochrin. (B) Anti-HCV effects of the sulochrin derivatives (10, 30, and 50 μM) were investigated as shown in Fig. 1C. (C) The $IC_{50}$ and $CC_{50}$ values of the sulochrin derivatives are shown.

first report to demonstrate the antiviral activity of these compounds. It is important to note that sulochrin inhibited the entry of HCV genotype 1a and b, which are the dominant genotypes in North America, Europe, and East Asia, indicating that this compound has potential clinical applications. Promising applications of entry inhibitors include the prevention of HCV recurrence in patients after liver transplantation. In patients with HCV-related end-stage liver diseases undergoing liver transplantation, re-infection of the graft is universal and characterised by accelerated progression of liver diseases. Entry inhibitors may be effective especially in these conditions under robust re-infection of HCV into hepatocytes. In the present study, we showed that co-treatment of sulochrin with IFNα and a protease inhibitor, teleprevir, synergistically augmented the anti-HCV effects of these approved drugs. These results suggest the possibility that co-treatment with sulochrin and probably its effective derivatives helps to inhibit the spread of HCV infection. We also identified the chemical structure and the derivatives of sulochrin as lead compounds for anti-HCV agents. Further derivatives analysis may identify more preferable anti-HCV agents.

In conclusion, our results demonstrate that sulochrin and its derivatives are potent and selective inhibitors of HCV infection in cell culture. Although further studies including an analysis of mode of action and pharmacological properties *in vivo* are required, this class of compounds should be pursued for its clinical potential in the treatment of HCV infection.

## Acknowledgments

Huh-7.5.1 cells were kindly provided by Dr. Francis Chisari at The Scripps Research Institute. The expression plasmids for producing HCVpp were a generous gift from Dr. Francois-Loic Cosset at Universite de Lyon. The expression plasmid for HCV E1E2 of genotype 1a (RMT) was kindly provided by Dr. Michinori Kohara at Tokyo Metropolitan Institute of Medical Science. We thank all of the members of the Department of Virology II, National Institute of Infectious Diseases, for their helpful discussions. This study was supported by grants-in-aid from the Ministry of Health, Labour, and Welfare, Japan, from the Ministry of Education, Culture, Sports, Science, and Technology, Japan, and from the Japan Society for the Promotion of Science.

## Appendix A. Supplementary data

Supplementary data associated with this article can be found, in the online version, at http://dx.doi.org/10.1016/j.bbrc.2013.09.100.

## References

[1] T.J. Liang, V. Rustgi, E. Galun, H.E. Blum, HCV RNA in patients with chronic hepatitis C treated with interferon-alpha, J. Med. Virol. 40 (1993) 69–75.
[2] J.G. McHutchison, S.C. Gordon, E.R. Schiff, M.L. Shiffman, W.M. Lee, V.K. Rustgi, Z.D. Goodman, M.H. Ling, S. Cort, J.K. Albrecht, Interferon alfa-2b alone or in combination with ribavirin as initial treatment for chronic hepatitis C. Hepatitis interventional therapy group, N. Engl. J. Med. 339 (1998) 1485–1492.
[3] A.W. Tai, R.T. Chung, Treatment failure in hepatitis C: mechanisms of non-response, J. Hepatol. 50 (2009) 412–420.
[4] V. Lohmann, F. Korner, J. Koch, U. Herian, L. Theilmann, R. Bartenschlager, Replication of subgenomic hepatitis C virus RNAs in a hepatoma cell line, Science 285 (1999) 110–113.
[5] B. Bartosch, J. Dubuisson, F.L. Cosset, Infectious hepatitis C virus pseudo-particles containing functional E1–E2 envelope protein complexes, J. Exp. Med. 197 (2003) 633–642.
[6] M. Hsu, J. Zhang, M. Flint, C. Logvinoff, C. Cheng-Mayer, C.M. Rice, J.A. McKeating, Hepatitis C virus glycoproteins mediate pH-dependent cell entry of pseudotyped retroviral particles, Proc. Natl. Acad. Sci. USA 100 (2003) 7271–7276.
[7] T. Wakita, T. Pietschmann, T. Kato, T. Date, M. Miyamoto, Z. Zhao, K. Murthy, A. Habermann, H.G. Krausslich, M. Mizokami, R. Bartenschlager, T.J. Liang, Production of infectious hepatitis C virus in tissue culture from a cloned viral genome, Nat. Med. 11 (2005) 791–796.
[8] J. Zhong, P. Gastaminza, G. Cheng, S. Kapadia, T. Kato, D.R. Burton, S.F. Wieland, S.L. Uprichard, T. Wakita, F.V. Chisari, Robust hepatitis C virus infection *in vitro*, Proc. Natl. Acad. Sci. USA 102 (2005) 9294–9299.
[9] B.D. Lindenbach, M.J. Evans, A.J. Syder, B. Wolk, T.L. Tellinghuisen, C.C. Liu, T. Maruyama, R.O. Hynes, D.R. Burton, J.A. McKeating, C.M. Rice, Complete replication of hepatitis C virus in cell culture, Science 309 (2005) 623–626.
[10] R. Suzuki, K. Saito, T. Kato, M. Shirakura, D. Akazawa, K. Ishii, H. Aizaki, Y. Kanegae, Y. Matsuura, I. Saito, T. Wakita, T. Suzuki, Trans-complemented hepatitis C virus particles as a versatile tool for study of virus assembly and infection, Virology 432 (2012) 29–38.
[11] G.M. Cragg, D.J. Newman, Natural products: a continuing source of novel drug leads, Biochim. Biophys. Acta 2013 (1830) 3670–3695.
[12] D.J. Newman, G.M. Cragg, Natural products as sources of new drugs over the 30 years from 1981 to 2010, J. Nat. Prod. 75 (2012) 311–335.
[13] A.L. Harvey, Natural products as a screening resource, Curr. Opin. Chem. Biol. 11 (2007) 480–484.
[14] S.S. Yang, G.M. Cragg, D.J. Newman, J.P. Bader, Natural product-based anti-HIV drug discovery and development facilitated by the NCI developmental therapeutics program, J. Nat. Prod. 64 (2001) 265–277.
[15] K. Kitazato, Y. Wang, N. Kobayashi, Viral infectious disease and natural products with antiviral activity, Drug Discovery Ther. 1 (2007) 14–22.
[16] K. Watashi, G. Liang, M. Iwamoto, H. Marusawa, N. Uchida, T. Daito, K. Kitamura, M. Muramatsu, H. Ohashi, T. Kiyohara, R. Suzuki, J. Li, S. Tong, Y. Tanaka, K. Murata, H. Aizaki, T. Wakita, Interleukin-1 and tumor necrosis factor-alpha trigger restriction of hepatitis B virus infection via a cytidine deaminase AID, J. Biol Chem. PMID: 24025329.
[17] Y. Myobatake, T. Takeuchi, K. Kuramochi, I. Kuriyama, T. Ishido, K. Hirano, F. Sugawara, H. Yoshida, Y. Mizushina, Pinophilins A and B, inhibitors of mammalian A-, B-, and Y-family DNA polymerases and human cancer cell proliferation, J. Nat. Prod. 75 (2012) 135–141.
[18] A. Murayama, N. Sugiyama, K. Watashi, T. Masaki, R. Suzuki, H. Aizaki, T. Mizuochi, T. Wakita, T. Kato, Japanese reference panel of blood specimens for evaluation of hepatitis C virus RNA and core antigen quantitative assays, J. Clin. Microbiol. 50 (2012) 1943–1949.
[19] K. Watashi, M. Khan, V.R. Yedavalli, M.L. Yeung, K. Strebel, K.T. Jeang, Human immunodeficiency virus type 1 replication and regulation of APOBEC3G by peptidyl prolyl isomerase Pin1, J. Virol. 82 (2008) 9928–9936.
[20] K. Watashi, M.L. Yeung, M.F. Starost, R.S. Hosmane, K.T. Jeang, Identification of small molecules that suppress microRNA function and reverse tumorigenesis, J. Biol. Chem. 285 (2010) 24707–24716.
[21] T. Kato, T. Date, M. Miyamoto, M. Sugiyama, Y. Tanaka, E. Orito, T. Ohno, K. Sugihara, I. Hasegawa, K. Fujiwara, K. Ito, A. Ozasa, M. Mizokami, T. Wakita, Detection of anti-hepatitis C virus effects of interferon and ribavirin by a sensitive replicon system, J. Clin. Microbiol. 43 (2005) 5679–5684.
[22] H. Marusawa, M. Hijikata, K. Watashi, T. Chiba, K. Shimotohno, Regulation of Fas-mediated apoptosis by NF-kappa B activity in human hepatocyte derived cell lines, Microbiol. Immunol. 45 (2001) 483–489.
[23] F. Yasui, M. Sudoh, M. Arai, M. Kohara, Synthetic lipophilic antioxidant BO-653 suppresses HCV replication, J. Med. Virol. 85 (2013) 241–249.
[24] M.B. Zeisel, I. Fofana, S. Fafi-Kremer, T.F. Baumert, Hepatitis C virus entry into hepatocytes: molecular mechanisms and targets for antiviral therapies, J. Hepatol. 54 (2011) 566–576.
[25] E. Blanchard, S. Belouzard, L. Goueslain, T. Wakita, J. Dubuisson, C. Wychowski, Y. Rouille, Hepatitis C virus entry depends on clathrin-mediated endocytosis, J. Virol. 80 (2006) 6964–6972.
[26] A. Codran, C. Royer, D. Jaeck, M. Bastien-Valle, T.F. Baumert, M.P. Kieny, C.A. Pereira, J.P. Martin, Entry of hepatitis C virus pseudotypes into primary human hepatocytes by clathrin-dependent endocytosis, J. Gen. Virol. 87 (2006) 2583–2593.
[27] L. Meertens, C. Bertaux, T. Dragic, Hepatitis C virus entry requires a critical postinternalisation step and delivery to early endosomes via clathrin-coated vesicles, J. Virol. 80 (2006) 11571–11578.
[28] D.K. Cureton, R.H. Massol, S.P. Whelan, T. Kirchhausen, The length of vesicular stomatitis virus particles dictates a need for actin assembly during clathrin-dependent endocytosis, PLoS Pathog. 6 (2010) e1001127.
[29] H.C. Huang, C.C. Chen, W.C. Chang, M.H. Tao, C. Huang, Entry of hepatitis B virus into immortalised human primary hepatocytes by clathrin-dependent endocytosis, J. Virol. 86 (2012) 9443–9453.
[30] H. Ohashi, M. Ishikawa, J. Ito, A. Ueno, G.J. Gleich, H. Kita, H. Kawai, H. Fukamachi, Sulochrin inhibits eosinophil degranulation, J. Antibiotechnol. (Tokyo) 50 (1997) 972–974.
[31] H. Ohashi, Y. Motegi, H. Kita, G.J. Gleich, T. Miura, M. Ishikawa, H. Kawai, H. Fukamachi, Sulochrin inhibits eosinophil activation and chemotaxis, Inflamm. Res. 47 (1998) 409–415.
[32] H.J. Lee, J.H. Lee, B.Y. Hwang, H.S. Kim, J.J. Lee, Fungal metabolites, asterric acid derivatives inhibit vascular endothelial growth factor (VEGF)-induced tube formation of HUVECs, J. Antibiotechnol. (Tokyo) 55 (2002) 552–556.
[33] R. Nicoletti, E. Manzo, M.L. Ciavatta, Occurence and bioactivities of funicone-related compounds, Int. J. Mol. Sci. 10 (2009) 1430–1444.

JACS
JOURNAL OF THE AMERICAN CHEMICAL SOCIETY
Article
pubs.acs.org/JACS

# Total Synthesis and Anti-Hepatitis C Virus Activity of MA026

Satomi Shimura,[†] Masahiro Ishima,[†] Syo Nakajima,[†,‡] Toshitaka Fujii,[†] Natsumi Himeno,[†] Kentaro Ikeda,[†] Jesus Izaguirre-Carbonell,[†] Hiroshi Murata,[†] Toshifumi Takeuchi,[†] Shinji Kamisuki,[†] Takahiro Suzuki,[§] Kouji Kuramochi,[∥] Koichi Watashi,[†,‡] Susumu Kobayashi,[§] and Fumio Sugawara*[,†]

[†]Department of Applied Biological Science, Tokyo University of Sciences, Noda, Chiba 278-8510, Japan
[‡]Department of Virology II, National Institute of Infectious Diseases, Shinjuku-ku, Tokyo 162-8640, Japan
[§]Faculty of Pharmaceutical Sciences, Tokyo University of Science, Noda, Chiba 278-8510, Japan
[∥]Graduate School of Life and Environmental Sciences, Kyoto Prefectural University, Sakyo-ku, Kyoto 606-8522, Japan

Supporting Information

**ABSTRACT:** The first total synthesis of MA026 and the identification of its candidate target protein for anti-hepatitis C virus activity are presented. MA026, a novel lipocyclodepsipeptide isolated from the fermentation broth of *Pseudomonas* sp. RtIB026, consists of a cyclodepsipeptide, a chain peptide, and an N-terminal (*R*)-3-hydroxydecanoic acid. The first subunit, side chain **2**, was prepared by coupling fatty acid moiety **4** with tripeptide **5**. The key macrocyclization of the decadepsipeptide at L-Leu[10]-D-Gln[11] provided the second subunit, cyclodepsipeptide **3**. Late-stage condensation of the two key subunits and final deprotection afforded MA026. This convergent, flexible, solution-phase synthesis will be invaluable in generating MA026 derivatives for future structure–activity relationship studies. An infectious hepatitis C virus (HCV) cell culture assay revealed that MA026 suppresses HCV infection into host hepatocytes by inhibiting the entry process in a dose-dependent manner. Phage display screening followed by surface plasmon resonance (SPR) binding analyses identified claudin-1, an HCV entry receptor, as a candidate target protein of MA026.

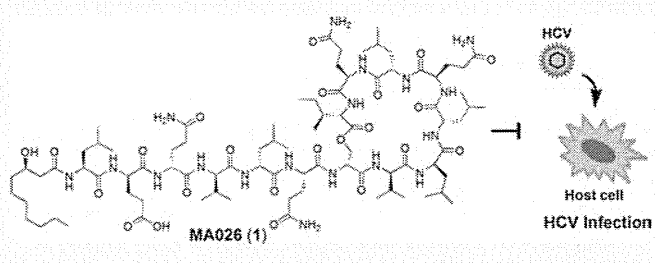


## INTRODUCTION

MA026 (**1**) (Figure 1),[1] a novel lipocyclodepsipeptide, exhibits antiviral activity against hepatitis C virus (HCV). HCV, a member of the *Flaviviridae* family, is a major causative agent of chronic liver diseases such as liver cirrhosis and hepatocellular carcinoma[2] and is thought to affect more than 170 million individuals worldwide, resulting in approximately 280 000 deaths per year.[3] Unfortunately, antiviral treatments consisting of PEGylated interferon (IFN) in combination with ribavirin and newly approved protease inhibitors are limited by serious adverse effects. The emergence of drug-resistant viruses and the high cost of current treatment regimens has led to an urgent search for alternative approaches to prevent HCV infection.[4] The life cycle of HCV includes entry into the host cell (entry process), uncoating of the viral genome, translation of viral proteins, viral genome replication, and the assembly and release of viral particles.[5] The recent development of an HCV cell culture system facilitated the elucidation of the viral replication machinery.[6] Identification of anti-HCV compounds, such as MA026, may be important in establishing novel strategies to inhibit HCV infection.

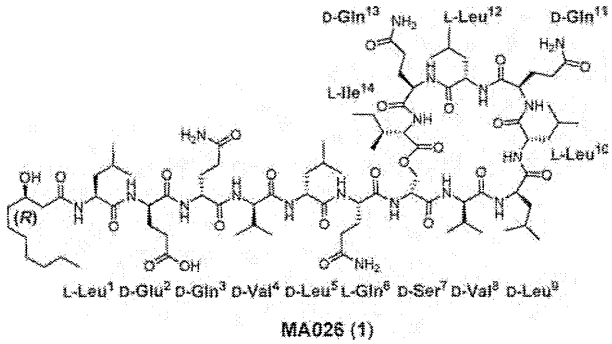


**Figure 1.** Chemical structure of MA026 (**1**).

MA026 (**1**) was isolated from the fermentation broth of *Pseudomonas* sp. RtIB026 found in the digestive tract of rainbow trout (*Oncorhynchus mykiss*).[1] Rainbow trout, an important aquaculture species, is known to be highly susceptible to infectious hematopoietic necrosis virus (IHN-V).[7] IHNV, a member of the genus *Novirhabdovirus* in the Rhabdoviridae family, is a causative agent of infectious hematopoietic necrosis (IHN), which is one of the most serious infectious diseases of salmonids.[8] An outbreak of IHNV in rainbow trout aquaculture can cause extensive economic loss.[9] For this reason, surveys were conducted on farmed rainbow trout that identified individual fish resistant to IHNV infection. Our previous studies revealed that rainbow trout with

**Received:** October 3, 2013

   dx.doi.org/10.1021/ja410145x | J. Am. Chem. Soc. XXXX, XXX, XXX–XXX

Scheme 1. Retrosynthetic Analysis of MA026 (1)

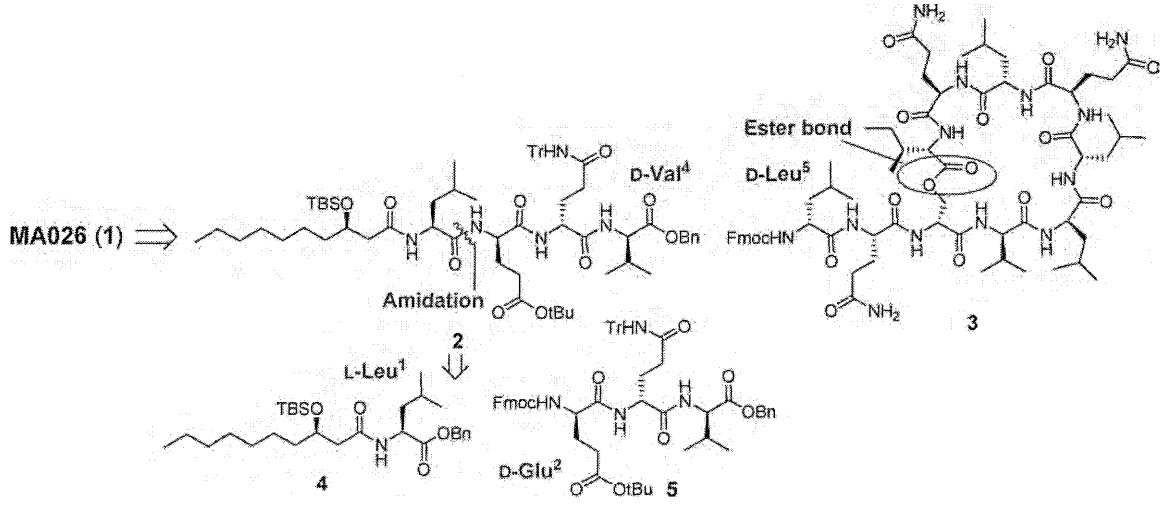


resistance to IHNV infection live in symbiosis with *Pseudomonas* sp. RtIB026 in their digestive tracts.[1] Anti-IHNV bioassay-guided fractionation of organic extracts from the culture fluid of *Pseudomonas* sp. RtIB026 resulted in the isolation of a new lipocyclodepsipeptide, designated MA026, as a principal active constituent.

The structure of MA026 was established in 2002[1] by amino acid composition analyses and NMR analyses with chemical modifications. MA026 was found to consist of a cyclodepsipeptide composed of eight amino acids, a chain peptide composed of six amino acids, and an N-terminal (*R*)-3-hydroxydecanoic acid. In total, MA026 contains 14 amino acids, nine of which possess the D configuration, as shown by HPLC analyses using Marfey's reagent. The amino acid sequence was determined by MS/MS analyses and comparison of partial peptide segments obtained by degradation of the natural product with synthetic peptides. The cyclodepsipeptide comprises a 25-membered ring in which the carboxylic group of L-Ile[14] forms a lactone bond with the hydroxy group of D-Ser.[7] To date, a wide range of lipocyclodepsipeptides have been identified,[10] including xantholysin A, an analogue of MA026.[11] In terms of sequence, xantholysin A differs from MA026 by two amino acids, namely, Gln[10]-Leu[11] in xantholysin A versus L-Leu[10]-D-Gln[11] in MA026. However, absolute configurations at all stereogenic centers in xantholysin A have yet to be determined.

In common with a number of lipocyclodepsipeptides, MA026 possesses a complex structure and interesting biological activity. In particular, MA026 displays anti-HCV activity that could be used to develop a novel antiviral drug. However, in order to reveal the mechanism of this anti-HCV activity, it is essential to develop a flexible chemical synthesis of MA026 to facilitate chemical modification of its structure. Herein we describe the first total synthesis of MA026 (**1**). Using a HCV cell culture assay, we have clarified that MA026 inhibits the HCV entry process into a hepatocyte cell line. Moreover, phage display screening and surface plasmon resonance (SPR) binding analyses suggested that MA026 might interact with claudin-1 (CLDN1), a cellular entry receptor of HCV.

## RESULTS AND DISCUSSION

**Retrosynthetic Analysis.** MA026 (**1**) was divided into two key segments to maximize the convergency of the synthesis: side chain **2** and cyclodepsipeptide **3** (Scheme 1). The cyclodepsipeptide contains a lactone bond composed of the carboxylic group of L-Ile[14] and the hydroxy group of D-Ser.[7] We envisaged a potential exchange of an ester bond with an amide bond by attack of a free N-terminal amine located proximal to the ester linkage.[12] To prevent such an exchange, it is necessary to maintain a sufficient distance between the ester bond and the N-terminus of the cyclodepsipeptide. Therefore, **3** should contain the cyclodepsipeptide plus an additional two amino acids, with the coupling site of **2** and **3** chosen to be D-Val[4]-D-Leu[5]. The side chain **2** was separated between L-Leu[1] and D-Glu[2] to give fatty acid moiety **4** and tripeptide **5**.

Key to the synthesis of cyclodepsipeptide **3** was the macrocyclization of a decapeptide (Scheme 2). Because it is more difficult to construct an ester bond than an amide bond,[13] we decided to disconnect the macrocycle at an amide bond and construct an ester bond in the early stage of the synthesis. The macrocyclization site was chosen at L-Leu[10]-D-Gln[11] considering the steric hindrance due to the isopropyl group of Val or the isobutyl group of Leu. The macrocyclization substrate, decadepsipeptide **6**, was to be prepared by the joining of hexadepsipeptide **7** with two dipeptides.

In the course of the construction of several peptide fragments, selective protection and deprotection of specific functional groups are critical. The Fmoc group was employed to protect the N-terminal amines of cyclodepsipeptide **3** and tripeptide **5**. The orthogonal Boc group was used to protect the N-terminal amines of other peptides. We also introduced a trityl (Tr) protecting group for the side-chain amides of D-Gln[3] and L-Gln[6] to maintain the solubility of the peptides in several organic solvents. In particular, the Tr group plays a significant role in affording solubility for peptides in aprotic solvents such as THF. During the preparation of Tr-protected Gln, an amine was protected with an Alloc group, as this protective group could be selectively removed using a palladium catalyst without affecting the Tr group.

**Synthesis of Side Chain 2.** We began our synthetic efforts by targeting fatty acid moiety **4** (Scheme 3). Protection of alcohol **8**[14] with a *tert*-butyldimethylsilyl (TBS) group afforded (*R*)-3-hydroxycarboximide **9** in 97% yield. The chiral auxiliary of **9** was hydrolyzed (58% yield), and the resulting carboxylic acid was then coupled with TsOH·L-Leu-OBn to provide fatty acid moiety **4** in 66% yield.


dx.doi.org/10.1021/ja410145x | J. Am. Chem. Soc. XXXX, XXX, XXX–XXX

**Scheme 2. Retrosynthetic Analysis of Cyclodepsipeptide 3**

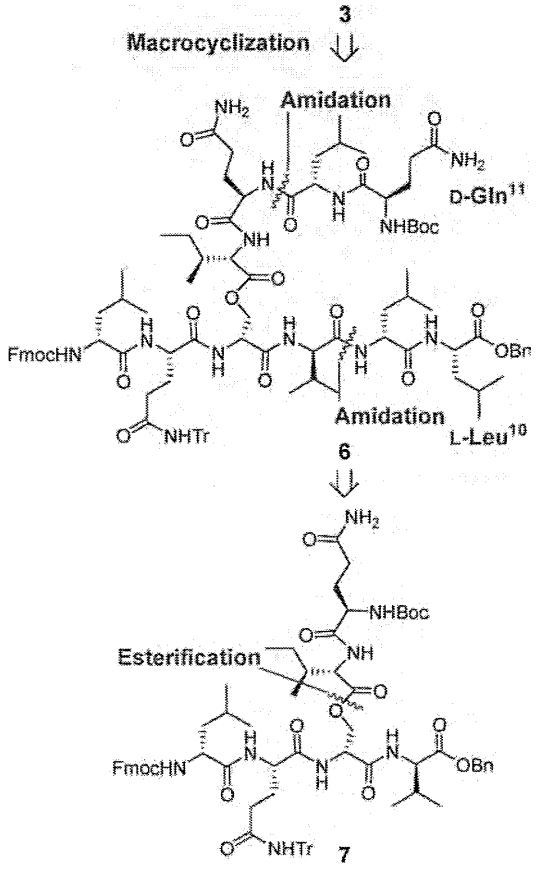


**Scheme 3. Synthesis of Fatty Acid Moiety 4**

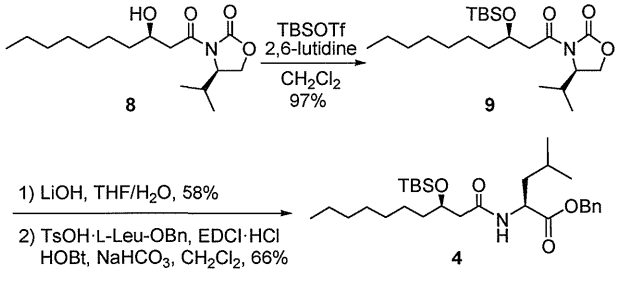


Tripeptide **5** was assembled as follows (Scheme 4). Alloc-D-Gln-OH (**10**) was treated with trityl alcohol and acetic anhydride under acidic conditions[15] to give the side-chain-protected residue in 66% yield. Subsequent condensation of this product with TsOH·D-Val-OBn provided dipeptide **11** in 81% yield. The Alloc group of **11** was then removed in the presence of a palladium catalyst and dimethylamine borane[16] (89% yield), and the resulting amine residue was coupled with Fmoc-D-Glu(O*t*Bu)-OH to afford **5** in 87% yield.

**Scheme 4. Preparation of Tripeptide 5**

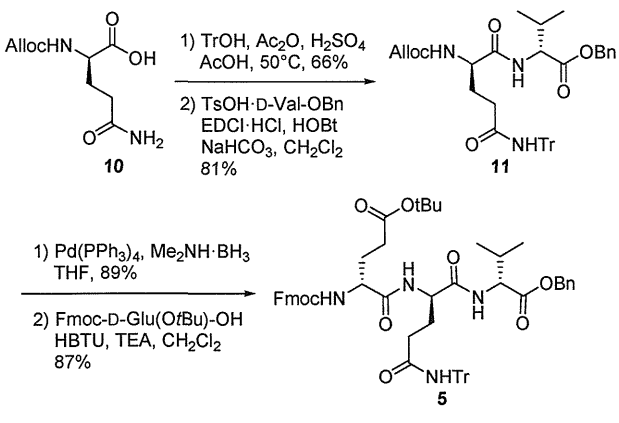


With fatty acid moiety **4** and tripeptide **5** in hand, we tried to link them together to obtain side chain **2** (Scheme 5).

**Scheme 5. Synthesis of Side Chain 2**

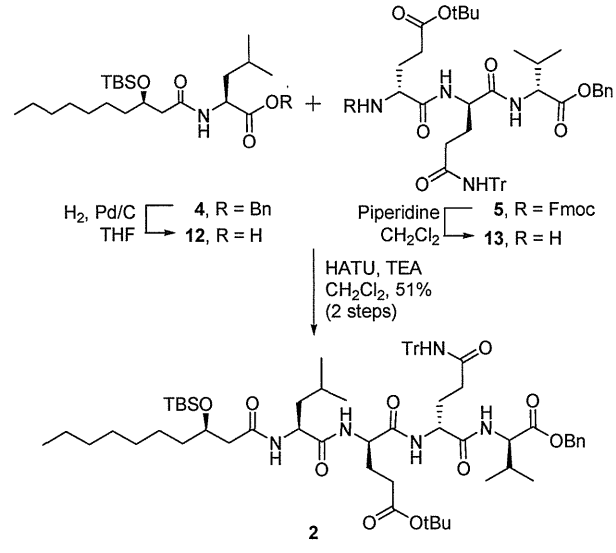


Hydrogenolysis of the benzyl ester in **4** gave carboxylic acid **12**, and cleavage of the Fmoc group in **5** by treatment with piperidine provided amine **13**.[17] Condensation of **12** with **13** in the presence of 2-(1*H*-7-azabenzotriazol)-1-yl-1,1,3,3-tetramethyluronium hexafluorophosphate (HATU) and triethylamine (TEA) afforded side chain **2** in 51% yield over the two steps.

**Synthesis of Cyclodepsipeptide 3.** The synthesis of the other key subunit, cyclodepsipeptide **3**, started with the construction of hexadepsipeptide **7**, an intermediate leading to the macrocyclization substrate, decadepsipeptide **6** (Scheme 6). To assemble **7** efficiently, three dipeptides were prepared as follows. Alloc-L-Gln-OH (**14**)[18] was treated with benzyl bromide and 1,8-diazabicycloundec-7-ene (DBU) to give the benzyl ester in 92% yield. Subsequent side-chain protection with a Tr group (86% yield) and removal of the Alloc group were performed by the same procedure as described earlier to give amine residue **15** in 94% yield. Condensation of **15** with Fmoc-D-Leu (93% yield) followed by hydrogenolysis of the benzyl ester afforded the corresponding dipeptide carboxylic acid **16** in 98% yield. Boc-D-Ser[19] and D-Val-OBn were coupled (92% yield), and cleavage of the carbamate linkage under acidic conditions furnished the corresponding dipeptide amine **17** in quantitative yield. Condensation of Boc-D-Gln with L-Ile-OBn (95% yield) and subsequent benzyl ester hydrogenolysis provided the corresponding dipeptide carboxylic acid **18** in 92% yield. Coupling of **16** with **17** in the presence of *O*-(benzotriazol-1-yl)-*N*,*N*,*N*′,*N*′-tetramethyluronium hexafluorophosphate (HBTU) and TEA afforded tetrapeptide **19** in 90% yield. The key esterification of the hindered alcohol of **19** with dipeptide carboxylic acid **18** was problematic. A wide range of procedures were examined, including the use of 1-(3-dimethylaminopropyl)-3-ethylcarbodiimide hydrochloride


dx.doi.org/10.1021/ja410145x | J. Am. Chem. Soc. XXXX, XXX, XXX–XXX

**Scheme 6. Construction of Hexadepsipeptide 7**

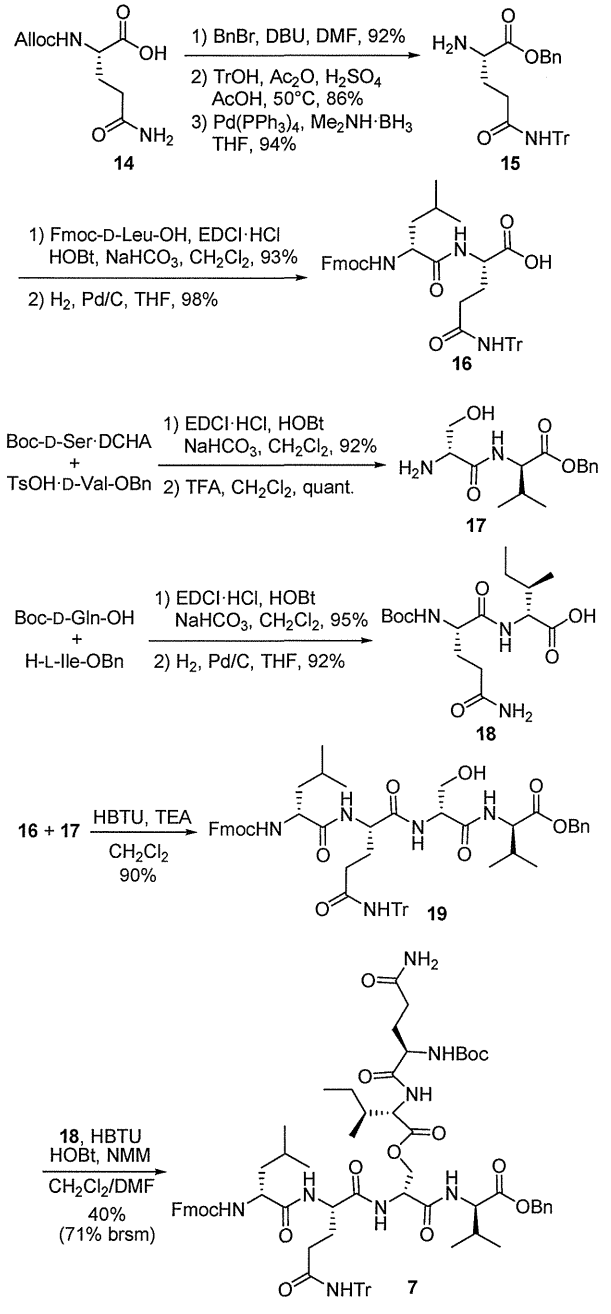


**Scheme 7. Synthesis of Decadepsipeptide 6**

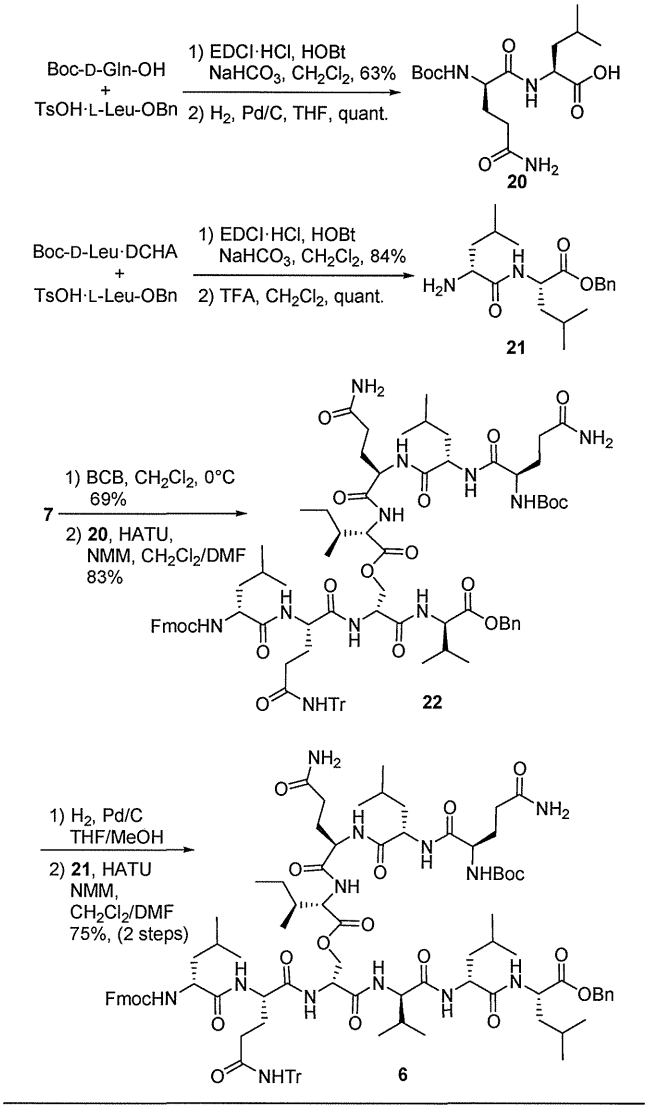


(EDCI), reactive mixed-anhydride activations, Yamaguchi esterification,[20] the Mukaiyama reagent,[21] and the Shiina reagent.[22] An esterification with EDCI, 1-hydroxybenzotriazole (HOBt) and *N*-methylmorpholine (NMM) resulted in low conversion, while the other protocols yielded no detectable product. Finally, esterification of **19** with **18** was successfully achieved in the presence of HBTU, HOBt, and NMM to afford hexadepsipeptide **7** in 40% yield (71% brsm).

With hexadepsipeptide **7** assembled, we turned our attention to the synthesis of decadepsipeptide **6** (Scheme 7). Two dipeptides **20** and **21**, components of **6**, were prepared as described below. Condensation of Boc-D-Gln with L-Leu-OBn (63% yield) followed by benzyl ester hydrogenolysis gave the corresponding dipeptide carboxylic acid **20** in quantitative yield. Boc-D-Leu and L-Leu-OBn were coupled (84% yield), and removal of the Boc group under acidic conditions provided the corresponding dipeptide amine **21** in quantitative yield. The next step was the incorporation of these dipeptides into hexadepsipeptide **7**. Selective removal of the Boc group of **7** without affecting the Tr group was accomplished by treatment with *B*-bromocatecholborane (BCB)[23] in $CH_2Cl_2$ in 69% yield, and the resulting hexadepsipeptide amine was coupled with **20** in the presence of HATU and NMM to afford octadepsipeptide **22** in 83% yield. Next, benzyl ester hydrogenolysis of **22** was performed. However, an unexpected cleavage of the Fmoc group was observed when this reaction was conducted in methanol (MeOH). In the case of another benzyl ester hydrogenolysis that provided dipeptide carboxylic acid **16** (Scheme 6), the Bn group was removed without the cleavage of the Fmoc group in tetrahydrofuran (THF). Octadepsipeptide **22** was difficult to dissolve in a moderately polar aprotic solvent such as THF, while the dipeptide described above dissolved with ease. This problem was resolved by introducing a 3:1 mixture of THF and MeOH as the solvent and adjusting the reaction time to allow complete benzyl ester hydrogenolysis.[24] Removal of the Bn group of **22** in 3:1 THF/MeOH provided the corresponding carboxylic acid. Subsequent coupling with **21** afforded decadepsipeptide **6** in 75% yield over the two steps.


dx.doi.org/10.1021/ja410145x | J. Am. Chem. Soc. XXXX, XXX, XXX–XXX

Having successfully obtained the macrocyclization substrate decadepsipeptide **6**, we next examined the cleavage of the Boc, Bn, and Tr groups and the subsequent intramolecular macrocyclization (Scheme 8). First, the Boc and Tr groups of **6** were removed under acidic conditions to provide the corresponding decadepsipeptide amine. The resulting product was next subjected to benzyl ester hydrogenolysis. However, it proved difficult to remove the benzyl ester selectively without affecting the Fmoc group because the decadepsipeptide amine dissolved in polar protic solvents such as MeOH or mixed solvents of THF/MeOH containing MeOH at a higher rate. Therefore, the deprotection sequence was changed. Benzyl ester hydrogenolysis of **6** proceeded in 1:1 THF/MeOH to provide the corresponding decadepsipeptide carboxylic acid, and then the Boc and Tr groups were removed with trifluoroacetic acid (TFA) in $CH_2Cl_2$ to afford the macrocyclization precursor.[25] At the stage of macrocyclization, reactions were performed under high-dilution conditions by slow addition of the substrate using a syringe pump in order to prevent the intermolecular reaction. We conducted the macrocyclization reaction with several coupling reagents,[26] including HATU, (benzotriazol-1-yloxy)tris(dimethylamino)-phosphonium hexafluorophosphate (BOP), (benzotriazol-1-yloxy)tripyrrolidinophosphonium hexafluorophosphate (PyBop), and (7-azabenzotriazol-1-yloxy)-tripyrrolidinophosphonium hexafluorophosphate (PyAOP). The protocol using PyAOP and 4-dimethylaminopyridine (DMAP) in DMF was found to promote the closure of the 25-membered ring to afford cyclodepsipeptide **3** in 18% yield over the three steps.

**Scheme 8. Synthesis of Cyclodepsipeptide 3**

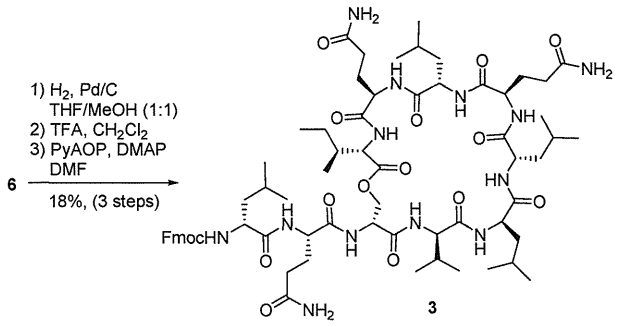


**Total Synthesis of MA026.** With the two required key segments (side chain **2** and cyclodepsipeptide **3**) in hand, we sought to link them together to accomplish the synthesis of MA026 (**1**) (Scheme 9). Removal of the N-terminal Fmoc group of **3** proceeded with diethylamine in DMF to provide the corresponding cyclodepsipeptide amine **24**. An alternative deprotection with piperidine resulted in the formation of several side products that were difficult to separate from **24**. Benzyl ester hydrogenolysis of **2** and subsequent coupling with amine **24** in the presence of PyAOP and DMAP furnished **25**. Although the deprotection of **2** and **3** gave corresponding

**Scheme 9. Synthesis of MA026 (1)**

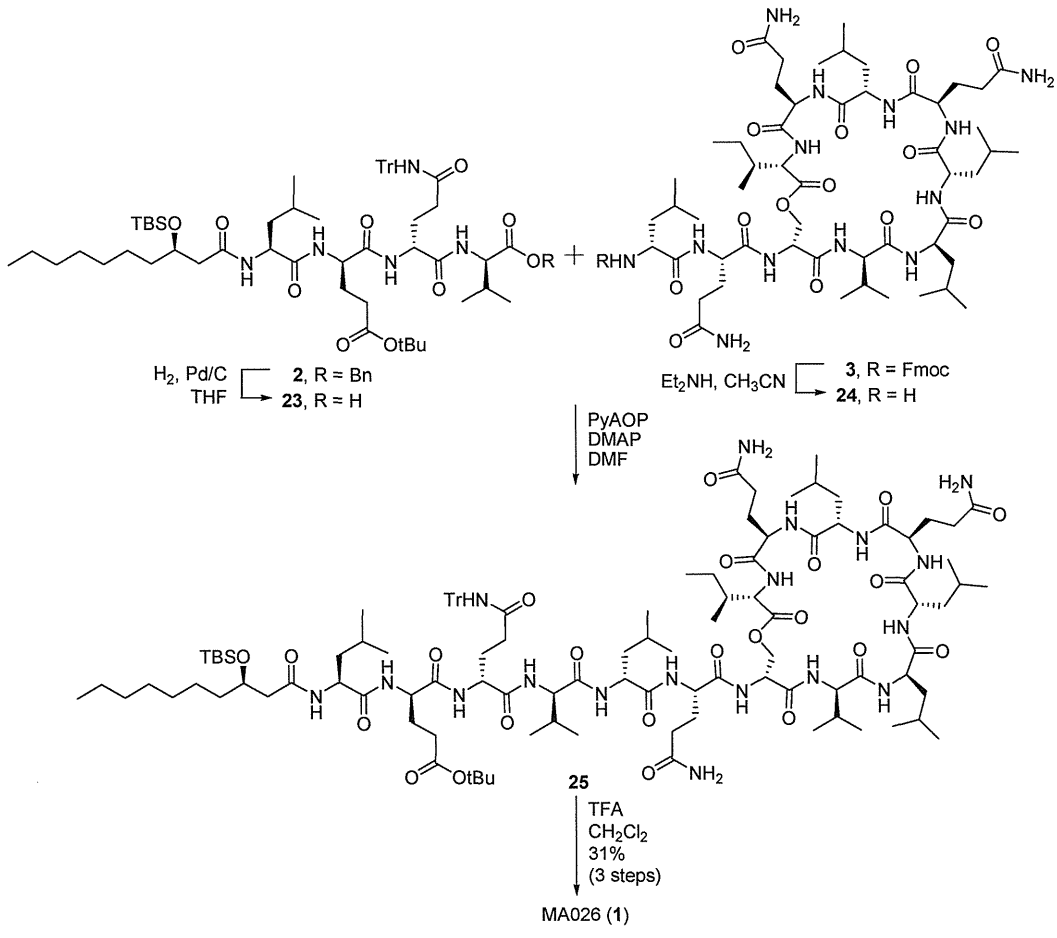



dx.doi.org/10.1021/ja410145x | J. Am. Chem. Soc. XXXX, XXX, XXX–XXX

carboxylic acid **23** and amine **24** in quantitative yield, their coupling did not proceed completely. Finally, a single-step cleavage of the Tr, *t*Bu, and TBS groups in **25** was achieved with TFA. The crude material was purified by reversed-phase HPLC to furnish pure **1** in 31% yield over the three steps. Analysis of synthetic **1** by $^{1}H$ and $^{13}C$ NMR spectroscopy, along with other spectroscopic data, showed it to be identical to the natural product.

**Anti-HCV Activity of MA026 (1).** MA026 shows antiviral activity against both IHNV and HCV. Given the fact that IHNV and HCV share a common entry process,[27,28] we reasoned that MA026 might inhibit the HCV entry process, which consists of cell binding, postcell binding, and endocytosis. On the basis of this prediction, we studied the anti-HCV activity of MA026 by measuring the HCV infectivity to determine whether MA026 inhibits the HCV entry process. Moreover, we compared the anti-HCV activity of synthetic **1** with that of the natural product (Figure 2).[29] Infectious HCV

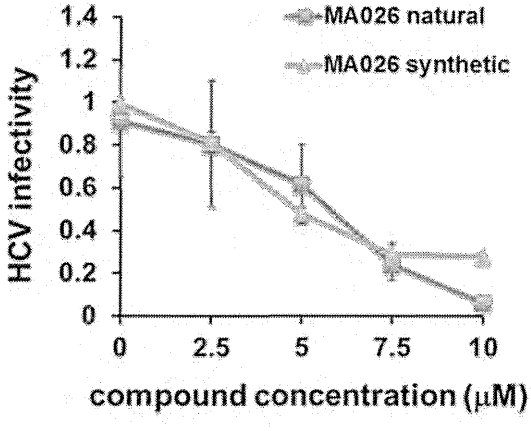


**Figure 2.** Evaluation of the anti-HCV activity of synthetic and natural **1**. The normalized infectivity was calculated as the HCV infectivity divided by the cell viability.

particles were pretreated with compounds for 1 h and infected into Huh-7.5.1 cells for 4 h. After residual virus and the test compound were washed out, cells were further cultured with growth medium in the absence of the compound for 72 h. The infectivity of HCV in the medium was quantified, and half-maximal inhibitory concentration ($IC_{50}$) values of the compounds were determined. In this assay, cells were exposed to the test compound only before and during HCV infection. Therefore, this pretreatment procedure could evaluate the potency of the test compound to inhibit the HCV entry process into the host cells. As shown in Figure 2, both synthetic **1** and the authentic natural product suppressed HCV infection into the host cells in a dose-dependent manner ($IC_{50}$ = 4.39 and 4.68 $\mu$M, respectively). Moreover, incubation in the presence of these compounds did not induce significant cytotoxicity within the concentration range used in these tests (Figure S1 in the Supporting Information). Thus, our data suggest that MA026 inhibits HCV infection by blocking the entry process. Phage display screening with immobilized MA026 and SPR binding analyses suggested claudin-1 as a candidate target for the anti-HCV activity of MA026.

To identify MA026 binding proteins, we applied a chemical biology approach and performed phage display screening.[30] Previously, we used phage display analyses to elucidate a novel mechanism of HCV replication by identifying the target protein of cyclosporin A.[31] Here we employed the same strategy to identify the target of MA026. MA026 was first immobilized on photoaffinity resin containing a photoactive diazirine group that we previously developed (Scheme S1 in the Supporting Information).[32,33] The mixture of photoafiinity resin and MA026 was irradiated with UV light. The highly reactive carbene induced by UV irradiation reacted with MA026, resulting in the production of immobilized MA026 in a nonspecific manner. Having prepared the MA026-immobilized resin, we then performed phage display screening using a random phage library displaying random peptides composed of 15 amino acids.[34] The phage display screening method is a powerful tool for identifying binding proteins of specific ligands. In this method, the phage library displaying peptides on phage particles (Input) was incubated with either MA026-immobilized resin or control resin (Bind) (Figure 3A and Figure S2A in the Supporting Information). Unbound phage particles were removed by washing (Selection). Phage particles bound to the MA026-immobilized resin were then eluted (Elute) and amplified in *Escherichia coli* (Amplify). The recovered phage clones (Input) were subsequently subjected to the next round of biopanning. Upon iteration of the biopanning cycles, the recovery rate of eluted phage clones compared with Input increased (Figure S2B). The relative enrichment of phage particles bound to MA026-immobilized resin was the highest upon the elution from the fourth round of biopanning (Figure 3B). Therefore, we randomly picked 27 single phage clones from the fourth-round elution. The sequence of peptides displayed on the phage particles, which were responsible for interaction with MA026, were determined from the DNA sequences of the corresponding phage vectors (Table S1 in the Supporting Information). Multiple sequence alignment analyses using CLUSTALW[35] indicated that peptides 1, 3, 10, 19, and 24 shared homology (Figure S3). Among them, we found the peptide sequence VFDSLL, a partially homologous sequence. We then searched the protein database using BLAST[36] to find proteins that showed similarities to the VFDSLL sequence. A single protein that includes the VFDSLL sequence, claudin-1 (CLDN1), was identified in the NCBI database. CLDN1 is highly expressed in the liver and plays an important role during the postcell binding process of HCV entry.[37]

On the basis of this knowledge and the result of phage display screenings followed by CLUSTALW and BLAST analyses, we proposed a hypothesis that MA026 might interact with CLDN1 and thereby suppress HCV infection. To confirm the interaction between CLDN1 and MA026, we performed SPR binding analyses using recombinant CLDN1 protein with an N-terminal glutathione S-transferase tag (CLDN1-GST). CLDN1-GST, or GST itself as a negative control, was first immobilized on a sensor chip of the SPR biosensor (Biacore 3000), and MA026 samples at different concentrations were then injected over the immobilized proteins.[38] The SPR data (Figure 3C) were subsequently analyzed to determine the dissociation constant ($K_D$). Our results showed a specific dose-dependent binding response of MA026 with CLDN1-GST ($K_D$ = 2.5 × $10^{-6}$ M). By contrast, the response with GST itself was significantly weaker ($K_D$ = 4.0 × $10^{-5}$ M). These results indicate a specific interaction between MA026 and recombinant CLDN1 protein.

The process of HCV entry into human hepatocytes requires the interaction of HCV glycoproteins E1 and E2 with host


dx.doi.org/10.1021/ja410145x | J. Am. Chem. Soc. XXXX, XXX, XXX–XXX

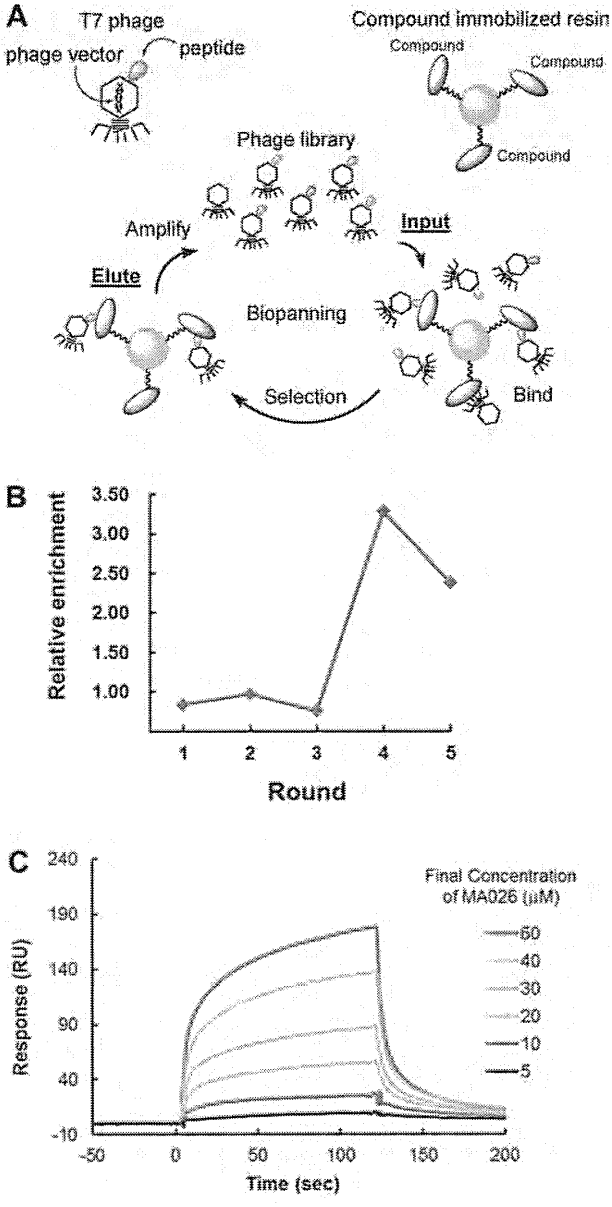


**Figure 3.** Phage display screenings and SPR analyses. (A) Procedure of phage display screening. (B) Relative enrichment of phage particles bound to MA026-immobilized resin. Relative enrichment was determined as the ratio of phage titer of elution from MA026-imobilized resin to phage titer of elution from control resin. (C) SPR analysis of binding between CLDN1-GST and MA026. Response units (RU) were calculated by subtracting the background response measured on the control flow cell from the response with the MA026 flow cell.

receptors, including tetraspanin CD81 and the high density lipoprotein receptor scavenger receptor class B type I (SR-BI).[39] It was reported that these two receptors are not sufficient for HCV entry and that more host proteins are involved.[40] CLDN1 is a transmembrane protein and belongs to a family of tight junction proteins that act as a barrier in cellular permeability.[41] It has been proposed that during the course of HCV entry, CLDN1 interacts with CD81 and influences the cell entry process, including endocytosis.[42] Although direct binding between HCV particles and CLDN1 has not been conclusively demonstrated, it has been shown that monoclonal anti-CLDN1 antibodies prevent HCV infection.[43] The peptide sequence VFDSLL, which is likely to interact with MA026, is conserved in the first extracellular loop (EL1) of CLDN1, and this loop is required for HCV entry.[37] The SPR analysis showed an interaction between MA026 and CLDN1-GST, and this result supports our hypothesis that MA026 might interact with CLDN1 and thereby prevent CLDN1 from interacting with CD81 and the HCV particle.

## CONCLUSIONS

The first total synthesis of MA026 was achieved in the solution phase with two key segments: side chain **2** and cyclodepsipeptide **3**. The construction of side chain **2** was accomplished with good efficiency by coupling of fatty acid moiety **4** with tripeptide **5**. In the preparation of macrocyclization substrate decadepsipeptide **6**, an appropriate choice of solvent was required to avoid the cleavage of the N-terminal Fmoc group through hydrogenolysis reactions. The key macrocyclization of the decadepsipeptide at L-Leu$^{10}$-D-Gln$^{11}$ was accomplished with PyAOP to afford **3**. This convergent modular synthetic route will be useful for the synthesis of a series of MA026 derivatives that will facilitate structure–activity relationship studies. Moreover, xantholysin A, an analogue of MA026, could be synthesized via this route once the stereochemistry is determined.

The anti-HCV activities of synthetic **1** and the authentic natural product were assessed and found to be similar. In this assay, the cells were exposed to the test compound only before and during HCV infection and then subsequently cultured in the absence of the test compound until sampling. Our results suggest that MA026 might inhibit the early step of HCV infection, including the cell entry process, rather than the following steps such as RNA replication and viral assembly and release. Phage display screenings were performed using MA026-immobilized resin and a random phage library. As the biopanning cycle was repeated, the ratio of phage clones bound to MA026 increased. We randomly picked 27 single phage clones and determined the peptide sequences displayed on the phage particles. From the results of multiple sequence alignment analyses using CLUSTALW, we found VFDSLL, a partially homologous peptide sequence. A BLAST search identified CLDN1 as a protein bearing the VFDSLL sequence. This protein plays an important role in the HCV entry process. The specific interaction between MA026 and recombinant CLDN1 protein was then confirmed by SPR analyses. Because the VFDSLL sequence is conserved in EL1 of CLDN1, we speculate that MA026 might interact with EL1 of CLDN1 and thereby interrupt HCV entry into the host cell.

Further investigations to develop an improved synthetic route that provides more efficient access to analogues and to reveal the detailed mechanism of the anti-HCV activity of MA026 are currently underway and will be disclosed in due course.

## ASSOCIATED CONTENT

### Supporting Information

Experimental procedures and analytical data for new compounds. This material is available free of charge via the Internet at http://pubs.acs.org.

## AUTHOR INFORMATION

### Corresponding Author

sugawara@rs.noda.tus.ac.jp


dx.doi.org/10.1021/ja410145x | J. Am. Chem. Soc. XXXX, XXX, XXX–XXX

## Notes

The authors declare no competing financial interest.

## ■ ACKNOWLEDGMENTS

We are grateful for the financial support of Toyo Suisan Kaisha, LTD., ADEKA Corporation, and a Sasakawa Scientific Research Grant from The Japan Science Society.

## ■ REFERENCES

(1) Ishima, M.; Yoshida, T.; Yamazaki, T.; Sugawara, F.; Hatta, K.; Shimojoe, M.; Masaki, K. PCT WO 02/062831, 2002.
(2) (a) Liang, T. J.; Jeffers, L. J.; Reddy, K. R.; Medina, M. D.; Parker, I. T.; Cheinquer, H.; Idrovo, V.; Rabassa, A.; Schiff, E. R. *Hepatology* **1993**, *18*, 1326–1333. (b) Lauer, G. M.; Walker, B. D. *N. Engl. J. Med.* **2001**, *345*, 41–52.
(3) Poynard, T.; Yuen, M. F.; Ratzin, V.; Lai, C. L. *Lancet* **2003**, *362*, 2095–2100.
(4) Tai, A. W.; Chung, R. T. *J. Hepatol.* **2009**, *50*, 412–420.
(5) Joyce, M. A.; Tyrrell, D. L. *J. Microbes Infect.* **2010**, *12*, 263–271.
(6) Wakita, T.; Pietschmann, T.; Kato, T.; Date, T.; Miyamoto, M.; Zhao, Z.; Murthy, K.; Habermann, A.; Kräusslich, H.; Mizokami, M.; Bartenschlager, R.; Liang, T. J. *Nat. Med. (New York, NY, U.S.)* **2005**, *11*, 791–796.
(7) Kim, H. J.; Oseko, N.; Nishizawa, T.; Yoshimizu, M. *Dis. Aquat. Org.* **2009**, *83*, 105–113.
(8) Wolf, K. Infectious Hematopoietic Necrosis. In *Fish Viruses and Fish Viral Disease*; Wolf, K., Ed.; Cornell University Press: Ithaca, NY, 1988; pp 83–114.
(9) Winton, J. R. *Annu. Rev. Fish Dis.* **1991**, *1*, 83–93.
(10) (a) Stolze, S. C.; Kaiser, M. *Molecules* **2013**, *18*, 1337–1367. (b) Andavan, G. S. B.; Lemmens-Gruber, R. *Mar. Drugs* **2010**, *8*, 810–834.
(11) Li, W.; Rokni-Zadeh, H.; Vleeschouwer, M. D.; Ghequire, M. G. K.; Sinnaeve, D.; Xie, G.; Rozenski, J.; Madder, A.; Martins, J. C.; Mot, R. D. *PLoS One* **2013**, *8*, No. e62946.
(12) Davies, J. S. *J. Pept. Sci.* **2003**, *9*, 471–501.
(13) Jiang, W.; Wanner, J.; Lee, R. J.; Bounaud, P.; Boger, D. L. *J. Am. Chem. Soc.* **2003**, *125*, 1877–1887.
(14) Alcohol **8** was synthesized by the asymmetric samarium-Reformatsky reaction of *n*-octylaldehyde with Evans' chiral 3-(2-bromoacetyl)-2-oxazolidinone. The overall yield of **8** was 48% over the two steps from Evans' chiral oxazolidinone. See: Fukuzawa, S.; Matsuzawa, H.; Yoshimitsu, S. *J. Org. Chem.* **2000**, *65*, 1702–1706.
(15) Boger, D. L.; Lee, R. J.; Bounaud, P.; Meier, P. *J. Org. Chem.* **2000**, *65*, 6770–6772.
(16) Gomez-Martinez, P.; Dessolin, M.; Guibé, F.; Albericio, F. *J. Chem. Soc., Perkin Trans. 1* **1999**, *1*, 2871–2874.
(17) Although hydrogenolysis of the benzyl ester in **4** gave carboxylic acid **12** in 94% yield, the cleavage of the Fmoc group in **5** gave amine **13** and some side products. See the Supporting Information for the synthesis of side chain **2**.
(18) Stevens, C. M.; Watanabe, R. *J. Am. Chem. Soc.* **1950**, *72*, 1877–1887.
(19) The preparation of Boc-D-Ser·DCHA is described in the Supporting Information.
(20) Inanaga, J.; Hirata, K.; Saeki, H.; Katsuki, T.; Yamaguchi, M. *Bull. Chem. Soc. Jpn.* **1979**, *52*, 1989–1993.
(21) Narasaka, K.; Maruyama, K.; Mukaiyama, T. *Chem. Lett.* **1978**, 885–888.
(22) (a) Shiina, I.; Ibuka, R.; Kubota, M. *Chem. Lett.* **2002**, 286–287. (b) Shiina, I.; Kubota, M.; Ibuka, R. *Tetrahedron Lett.* **2002**, *43*, 7535–7539.
(23) Boeckman, R. K, Jr.; Potenza, J. C. *Tetrahedron Lett.* **1985**, *26*, 1411–1414.
(24) In addition to the ratio of THF and MeOH, the amount of Pd/C was important to avoid the cleavage of the Fmoc group. The amount of Pd/C should be less than or equal to 0.1 equiv.
(25) The benzyl ester hydrogenolysis of **6** in 1:1 THF/MeOH gave the desired decadepsipeptide carboxylic acid, but the crude product included some peptides without the Fmoc group.
(26) (a) Han, S.; Kim, Y. *Tetrahedron* **2004**, *60*, 2447–2467. (b) Valeur, E.; Bradley, M. *Chem. Soc. Rev.* **2009**, *38*, 606–631.
(27) Liu, H.; Liu, Y.; Liu, S.; Pang, D.; Xiao, G. *J. Virol.* **2011**, *85*, 6252–6262.
(28) Blanchard, E.; Belouzard, S.; Goueslain, L.; Wakita, T.; Dubuisson, J.; Wychowski, C.; Rouillé, Y. *J. Virol.* **2006**, *80*, 6964–6972.
(29) Zhong, J.; Gastaminza, P.; Cheng, G.; Kapadia, S.; Kato, T.; Burton, D. R.; Wieland, S. F.; Uprichard, S. L.; Wakita, T.; Chisari, F. V. *Proc. Natl. Acad. Sci. U.S.A.* **2005**, *102*, 9294–9299.
(30) Smith, G. P.; Petrenko, V. A. *Chem. Rev.* **1997**, *97*, 391–410.
(31) Morohashi, K.; Sahara, H.; Watashi, K.; Iwabata, K.; Sunoki, T.; Kuramochi, K.; Takakusagi, K.; Miyashita, H.; Sato, N.; Tanabe, A.; Shimotohno, K.; Kobayashi, S.; Sakaguchi, K.; Sugawara, F. *PLoS One* **2011**, *6*, No. e18285.
(32) (a) Kanoh, N.; Honda, K.; Simizu, S.; Muroi, M.; Osada, H. *Angew. Chem., Int. Ed.* **2005**, *44*, 3559–3562. (b) Kuramochi, K.; Haruyama, T.; Takeuchi, R.; Sunoki, T.; Watanabe, M.; Oshige, M.; Kobayashi, S.; Sakaguchi, K.; Sugawara, F. *Bioconjugate Chem.* **2005**, *16*, 97–104.
(33) We used the natural product to prepare MA026-immobilized resin.
(34) Kusayanagi, T.; Tsukuda, S.; Shimura, S.; Manita, D.; Iwakiri, K.; Kamisuki, S.; Takakusagi, Y.; Takeuchi, T.; Kuramochi, K.; Nakazaki, A.; Sakaguchi, K.; Kobayashi, S.; Sugawara, F. *Bioorg. Med. Chem.* **2012**, *20*, 6248–6255.
(35) Thompson, J. D.; Higgins, D. G.; Gibson, T. J. *Nucleic Acids Res.* **1994**, *22*, 4673–4680.
(36) Altschul, S. F.; Madden, T. L.; Schäffer, A. A.; Zhang, J.; Zhang, Z.; Miller, W.; Lipman, D. J. *Nucleic Acids Res.* **1997**, *25*, 3389–3402.
(37) Evans, M. J.; von Hahn, T.; Tscherne, D. M.; Syder, A. J.; Panis, M.; Wölk, B.; Hatziioannou, T.; McKeating, J. A.; Bieniasz, P. D.; Rice, C. M. *Nature* **2007**, *446*, 801–805.
(38) In SPR analyses, we used the MA026 natural product.
(39) (a) Pileri, P.; Uematsu, Y.; Compagnoli, S.; Galli, G.; Falugi, F.; Petracca, R.; Weiner, A. J.; Houghton, M.; Rosa, D.; Grandi, G.; Abrignani, S. *Science* **1998**, *282*, 938–941. (b) Scarselli, E.; Ansuini, H.; Cerino, R.; Roccasecca, R. M.; Acali, S.; Filocamo, G.; Traboni, C.; Nicosia, A.; Cortese, R.; Vitelli, A. *EMBO J.* **2002**, *21*, 5017–5025.
(40) Bartosch, B.; Cosset, F. L. *Virology* **2006**, *348*, 1–12.
(41) Van Itallie, C. M.; Anderson, J. M. *Annu. Rev. Physiol.* **2006**, *68*, 403–429.
(42) Brazzoli, M.; Bianchi, A.; Filippini, S.; Weiner, A.; Zhu, Q.; Pizza, M.; Crotta, S. *J. Virol.* **2008**, *82*, 8316–8329.
(43) Krieger, S. E.; Zeisel, M. B.; Davis, C.; Thumann, C.; Harris, H. J.; Schnober, E. K.; Mee, C.; Soulier, E.; Royer, C.; Lambotin, M.; Grunert, F.; Thi, V. L. D.; Dreux, M.; Cosset, F.; McKeating, J. A.; Schuster, C.; Baumert, T. F. *Hepatology* **2010**, *51*, 1144–1157.


dx.doi.org/10.1021/ja410145x | J. Am. Chem. Soc. XXXX, XXX, XXX–XXX

*Journal of General Virology* (2014), **95**, 60–65 DOI 10.1099/vir.0.058008-0

Short Communication

# Production of single-round infectious chimeric flaviviruses with DNA-based Japanese encephalitis virus replicon

Ryosuke Suzuki,[1]† Tomohiro Ishikawa,[2]† Eiji Konishi,[3] Mami Matsuda,[1] Koichi Watashi,[1] Hideki Aizaki,[1] Tomohiko Takasaki[4] and Takaji Wakita[1]

Correspondence
Ryosuke Suzuki
ryosuke@nih.go.jp
Eiji Konishi
ekon@biken.osaka-u.ac.jp

[1]Department of Virology II, National Institute of Infectious Diseases, Toyama 1-23-1, Shinjuku-ku, Tokyo 162-8640, Japan

[2]Department of Microbiology, Dokkyo Medical University School of Medicine, 880 Kitakobayashi, Mibu-machi, Shimotsuga-gun, Tochigi, 321-0293, Japan

[3]BIKEN Endowed Department of Dengue Vaccine Development, Faculty of Tropical Medicine, Mahidol University, 420/6 Ratchawithi Road, Ratchahewi, Bangkok 10440, Thailand

[4]Department of Virology I, National Institute of Infectious Diseases, Toyama 1-23-1, Shinjuku-ku, Tokyo 162-8640, Japan

A method for rapid production of single-round infectious particles (SRIPs) of flavivirus would be useful for viral mutagenesis studies. Here, we established a DNA-based production system for SRIPs of flavivirus. We constructed a Japanese encephalitis virus (JEV) subgenomic replicon plasmid, which lacked the C-prM-E (capsid–pre-membrane–envelope) coding region, under the control of the cytomegalovirus promoter. When the JEV replicon plasmid was transiently co-transfected with a JEV C-prM-E expression plasmid into 293T cells, SRIPs were produced, indicating successful *trans*-complementation with JEV structural proteins. Equivalent production levels were observed when C and prM–E proteins were provided separately. Furthermore, dengue types 1–4, West Nile, yellow fever or tick-borne encephalitis virus prM-E proteins could be utilized for production of chimaeric flavivirus SRIPs, although the production was less efficient for dengue and yellow fever viruses. These results indicated that our plasmid-based system is suitable for investigating the life cycles of flaviviruses, diagnostic applications and development of safer vaccine candidates.

Received 1 August 2013
Accepted 3 October 2013

Japanese encephalitis virus (JEV) is the leading cause of viral encephalitis with severe mortality in eastern and south-eastern Asia, and is estimated to be responsible for 67 900 cases annually, mostly in children (Campbell *et al.*, 2011). The virus is transmitted by *Culex* mosquito vectors between pigs and/or wild birds, and humans and horses are thought to be dead-end hosts. JEV is a member of the genus *Flavivirus* within the family *Flaviviridae*, which includes dengue virus (DENV), West Nile virus (WNV), yellow fever virus (YFV) and tick-borne encephalitis virus (TBEV). JEV is an enveloped single-stranded positive-sense RNA virus with an 11 kb genome that is translated as a single large polyprotein. The polyprotein is co-translationally cleaved by host and viral proteases into three structural proteins – capsid (C), pre-membrane (prM) and envelope (E) – and seven non-structural (NS) proteins (Sumiyoshi *et al.*, 1987).

For several flaviviruses, subgenomic replicons, which lack structural protein genes but can replicate in cells, have been constructed (Khromykh & Westaway, 1997; Pang *et al.*, 2001; Shi *et al.*, 2002). In addition, the expression of viral structural proteins in cells harbouring replicon RNA has been shown to produce single-round infectious particles (SRIPs), which are infectious, but progeny viruses cannot be spread from the infected cells, as the packaged genome lacks structural protein genes (Gehrke *et al.*, 2003; Jones *et al.*, 2005; Khromykh *et al.*, 1998; Ng *et al.*, 2007; Scholle *et al.*, 2004; Yun *et al.*, 2009). Furthermore, *trans*-packaging of replicons by the prM-E proteins from heterologous flaviviruses have been reported (Ansarah-Sobrinho *et al.*, 2008; Yoshii *et al.*, 2008).

A method for rapidly producing SRIPs of flaviviruses would be useful for viral mutagenesis studies, diagnostic applications and the production of vaccines with reduced

†These authors contributed equally to this paper.

One supplementary figure is available with the online version of this paper.